

American Inventions in 21st Century

Trinity Hardwick



First Edition, 2012

ISBN 978-81-323-2715-8

WWT

© All rights reserved.

Published by:
Orange Apple
4735/22 Prakashdeep Bldg,
Ansari Road, Darya Ganj,
Delhi - 110002
Email: info@wtbooks.com

WORLD TECHNOLOGIES

Table of Contents

Chapter 1 - Wilkinson Microwave Anisotropy Probe

Chapter 2 - Segway PT

Chapter 3 - SERF

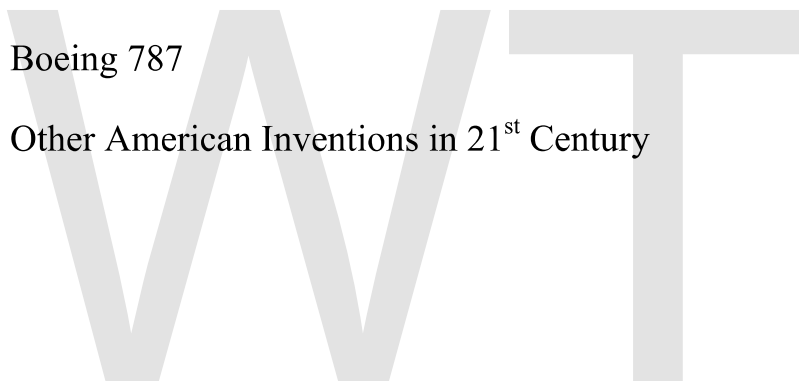
Chapter 4 - Fermionic Condensate

Chapter 5 - HPV Vaccine

Chapter 6 - Photosynth

Chapter 7 - Boeing 787

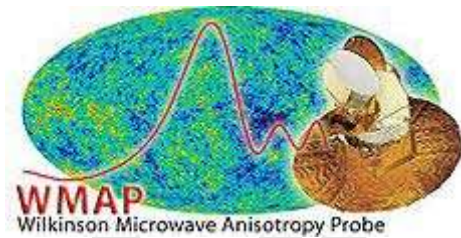
Chapter 8 - Other American Inventions in 21st Century



Chapter- 1

Wilkinson Microwave Anisotropy Probe

Wilkinson Microwave Anisotropy Probe



General information

NSSDC ID	2001-027A
Organization	NASA
Launch date	30 June 2001, 19:46 UTC
Launched from	Cape Canaveral Air Force Station
Launch vehicle	Delta II 7425-10
Mission length	9 years, 7 months, and 4 days elapsed
Mass	840 kg
Type of orbit	Lissajous orbit
Location	L ₂

Instruments

K-band 23 GHz	52.8 MOA beam
Ka-band 33 GHz	39.6 MOA beam
Q-band 41 GHz	30.6 MOA beam
V-band 61 GHz	21 MOA beam
W-band 94 GHz	13.2 MOA beam

The **Wilkinson Microwave Anisotropy Probe (WMAP)** — also known as the **Microwave Anisotropy Probe (MAP)**, and **Explorer 80** — is a spacecraft which measures differences in the temperature of the Big Bang's remnant radiant heat — the Cosmic Microwave Background Radiation — across the full sky. Headed by Professor Charles L. Bennett, Johns Hopkins University, the mission was developed in a joint partnership between the NASA Goddard Space Flight Center and Princeton University. The WMAP spacecraft was launched on 30 June 2001, at 19:46:46 GDT, from Florida. The WMAP mission succeeds the COBE space mission and was the second medium-class (MIDEX) spacecraft of the Explorer program. In 2003, MAP was renamed WMAP in honor of cosmologist David Todd Wilkinson (1935–2002), who had been a member of the mission's science team.

WMAP's measurements played the key role in establishing the current Standard Model of Cosmology. WMAP data are very well fit by a universe that is dominated by dark energy in the form of a cosmological constant. Other cosmological data are also consistent, and together tightly constrain the Model. In this Lambda-CDM model of the universe, the age of the universe is 13.75 ± 0.11 billion years. The WMAP mission's determination of the age of the universe to better than 1% precision was recognized by the Guinness Book of World Records. The current expansion rate of the universe is of $70.5 \pm 1.3 \text{ km}\cdot\text{s}^{-1}\cdot\text{Mpc}^{-1}$. The content of the universe presently consists of $4.56\% \pm 0.15\%$ ordinary baryonic matter; $22.8\% \pm 1.3\%$ Cold dark matter (CDM) that neither emits nor absorbs light; and $72.6\% \pm 1.5\%$ of dark energy in the form of a cosmological constant that accelerates the expansion of the universe. Less than 1% of the current contents of the universe is in neutrinos, but WMAP's measurements have found, for the first time in 2008, that the data prefers the existence of a cosmic neutrino background with an effective number of neutrino flavors of 4.4 ± 1.5 , consistent with the expectation of 3.06. The contents point to a "flat" Euclidean flat geometry, with the ratio of the energy density in curvature to the critical density $0.0179 < \Omega_k < 0.0081$ (95%CL). The WMAP measurements also support the cosmic inflation paradigm in several ways, including the flatness measurement.

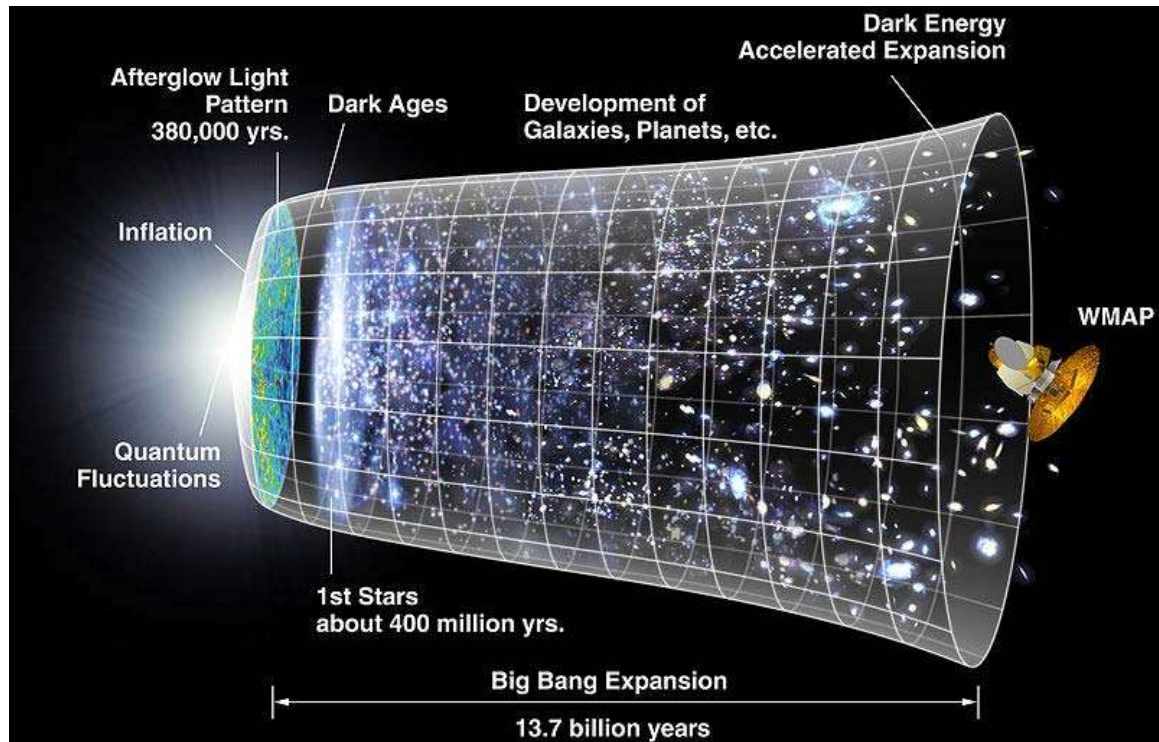
According to *Science* magazine, the WMAP was the *Breakthrough of the Year for 2003*. This mission's results papers were first and second in the "Super Hot Papers in Science Since 2003" list. Of the all-time most referenced papers in physics and astronomy in the SPIRES database, only three have been published since 2000, and all three are WMAP publications. On May 27, 2010, it was announced that Bennett, Lyman A. Page, Jr., and David N. Spergel, the latter both of Princeton University, would share the 2010 Shaw Prize in astronomy for their work on WMAP.

As of October 2010, the WMAP spacecraft is in a graveyard orbit after 9 years of operations. The Astronomy and Physics Senior Review panel at NASA Headquarters has endorsed a total of 9 years of WMAP operations, through September 2010. All WMAP data are released to the public and have been subject to careful scrutiny.

Some aspects of the data are statistically unusual for the Standard Model of Cosmology. For example, the greatest angular-scale measurements, the quadrupole moment, is

somewhat smaller than the Model would predict, but this discrepancy is not highly significant. A large cold spot and other features of the data are more statistically significant, and research continues into these.

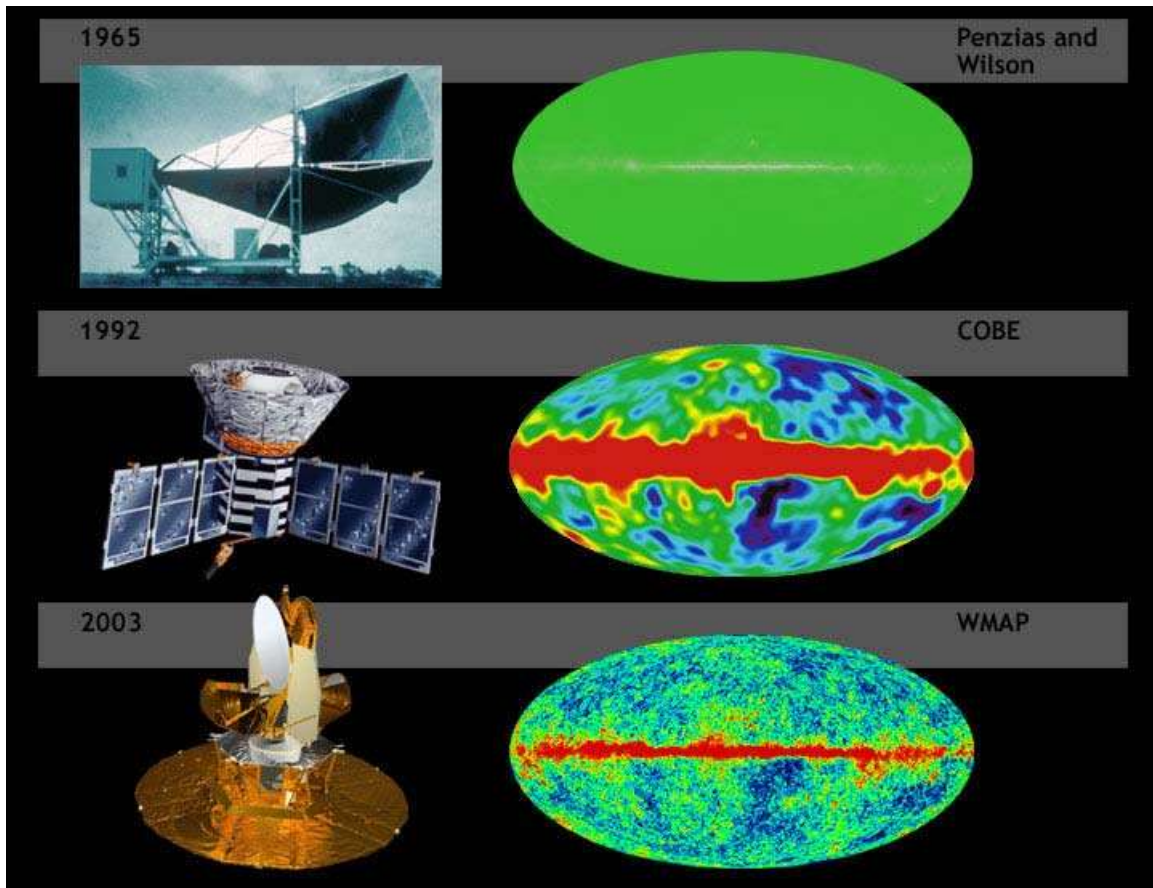
Objectives



The universe's timeline, from inflation to the WMAP

The WMAP objective is to measure the temperature differences in the Cosmic Microwave Background (CMB) radiation. The anisotropies then are used to measure the universe's geometry, content, and evolution; and to test the Big Bang model, and the cosmic inflation theory. For that, the mission is creating a full-sky map of the CMB, with a 13 arcminute resolution via multi-frequency observation. The map requires the fewest systematic errors, no correlated pixel noise, and accurate calibration, to ensure angular-scale accuracy greater than its resolution. The map contains 3,145,728 pixels, and uses the HEALPix scheme to pixelize the sphere. The telescope also measures the CMB's E-mode polarization, and foreground polarization; its life is 27 months; 3 to reach the L_2 position, 2 years of observation.

Development

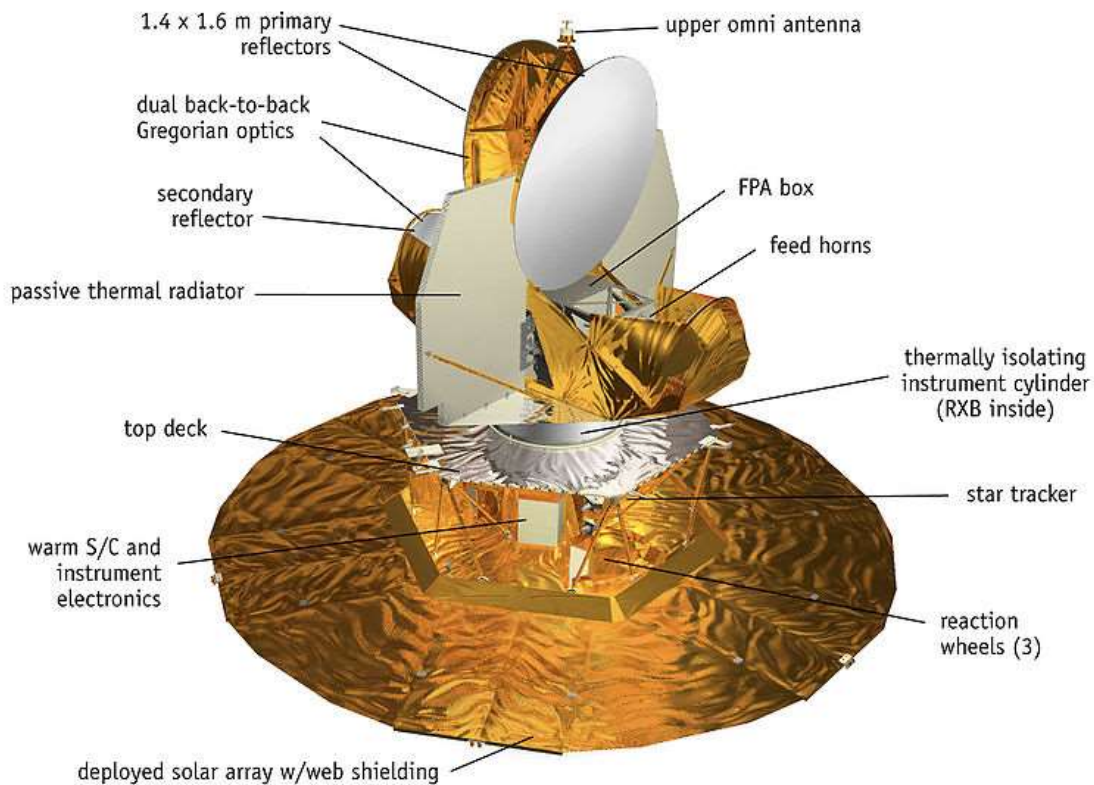


A comparison of the sensitivity of WMAP with COBE and Penzias and Wilson's telescope

The MAP mission was proposed to NASA in 1995, selected for definition study in 1996, and approved for development in 1997.

The WMAP was preceded by two missions to observe the CMB; (i) the Soviet RELIKT-1 that reported the upper-limit measurements of CMB anisotropies, and (ii) the U.S. COBE satellite that reported large-scale CMB fluctuations, and the ground-based and balloon experiments measuring the small-scale fluctuations in patches of sky: the Boomerang, the Cosmic Background Imager, and the Very Small Array. The WMAP is 45 times more sensitive, with 33 times the angular resolution of its COBE satellite predecessor.

Spacecraft



WMAP spacecraft diagram

The telescope's primary reflecting mirrors are a pair of Gregorian 1.4m x 1.6m dishes (facing opposite directions), that focus the signal onto a pair of 0.9m x 1.0m secondary reflecting mirrors. They are shaped for optimal performance: a carbon fibre shell upon a Korex core, thinly-coated with aluminium and silicon oxide. The secondary reflectors transmit the signals to the corrugated feedhorns that sit on a focal plane array box beneath the primary reflectors.

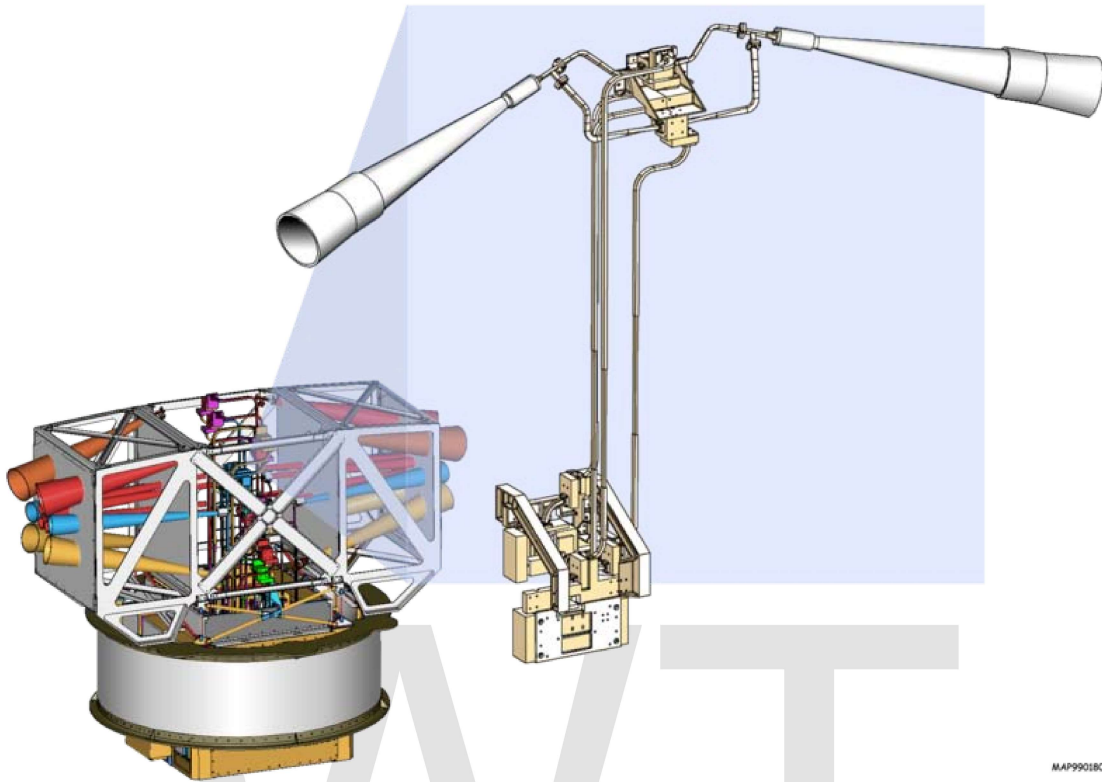


Illustration of WMAP's receivers

The receivers are polarization-sensitive differential radiometers measuring the difference between two telescope beams. The signal is amplified with HEMT low-noise amplifiers. There are 20 feeds, 10 in each direction, from which a radiometer collects a signal; the measure is the difference in the sky signal from opposite directions. The directional separation azimuth is 180 degrees; the total angle is 141 degrees. To avoid collecting Milky Way galaxy foreground signals, the WMAP uses five discrete radio frequency bands, from 23 GHz to 94 GHz.

Properties of WMAP at different frequencies

Property	K-band	Ka-band	Q-band	V-band	W-band
Central wavelength (mm)	13	9.1	7.3	4.9	3.2
Central frequency (GHz)	23	33	41	61	94

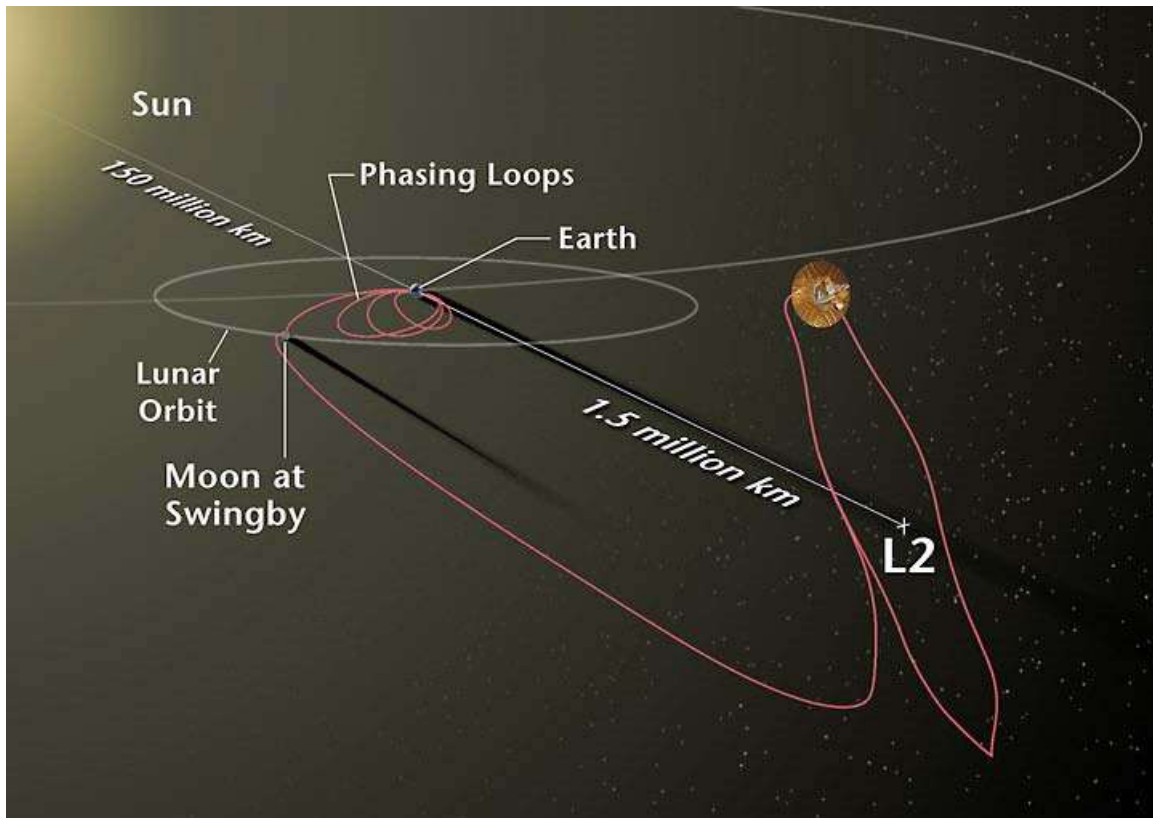
Bandwidth (GHz)	5.5	7.0	8.3	14.0	20.5
Beam size (arcminutes)	52.8	39.6	30.6	21	13.2
Number of radiometers	2	2	4	4	8
System temperature (K)	29	39	59	92	145
Sensitivity ($\text{mK s}^{1/2}$)	0.8	0.8	1.0	1.2	1.6

The WMAP's base is a 5.0m-diameter solar panel array that keeps the instruments in shadow during CMB observations, (by keeping the craft constantly angled at 22 degrees, relative to the sun). Upon the array sit a bottom deck (supporting the warm components) and a top deck. The telescope's cold components: the focal-plane array and the mirrors, are separated from the warm components with a cylindrical, 33 cm-long thermal isolation shell atop the deck.

Passive thermal radiators cool the WMAP to ca. 90 degrees K; they are connected to the low-noise amplifiers. The telescope consumes 419 W of power. The available telescope heaters are emergency-survival heaters, and there is a transmitter heater, used to warm them when off. The WMAP spacecraft's temperature is monitored with platinum resistance thermometers.

The WMAP's calibration is effected with the CMB dipole and measurements of Jupiter; the beam patterns are measured against Jupiter. The telescope's data are relayed daily via a 2 GHz transponder providing a 667kbit/s downlink to a 70m Deep Space Network telescope. The spacecraft has two transponders, one a redundant back-up; they are minimally active — ca. 40 minutes daily — to minimize radio frequency interference. The telescope's position is maintained, in its three axes, with three reaction wheels, gyroscopes, two star trackers and sun sensors, and is steered with eight hydrazine thrusters.

Launch, trajectory, and orbit

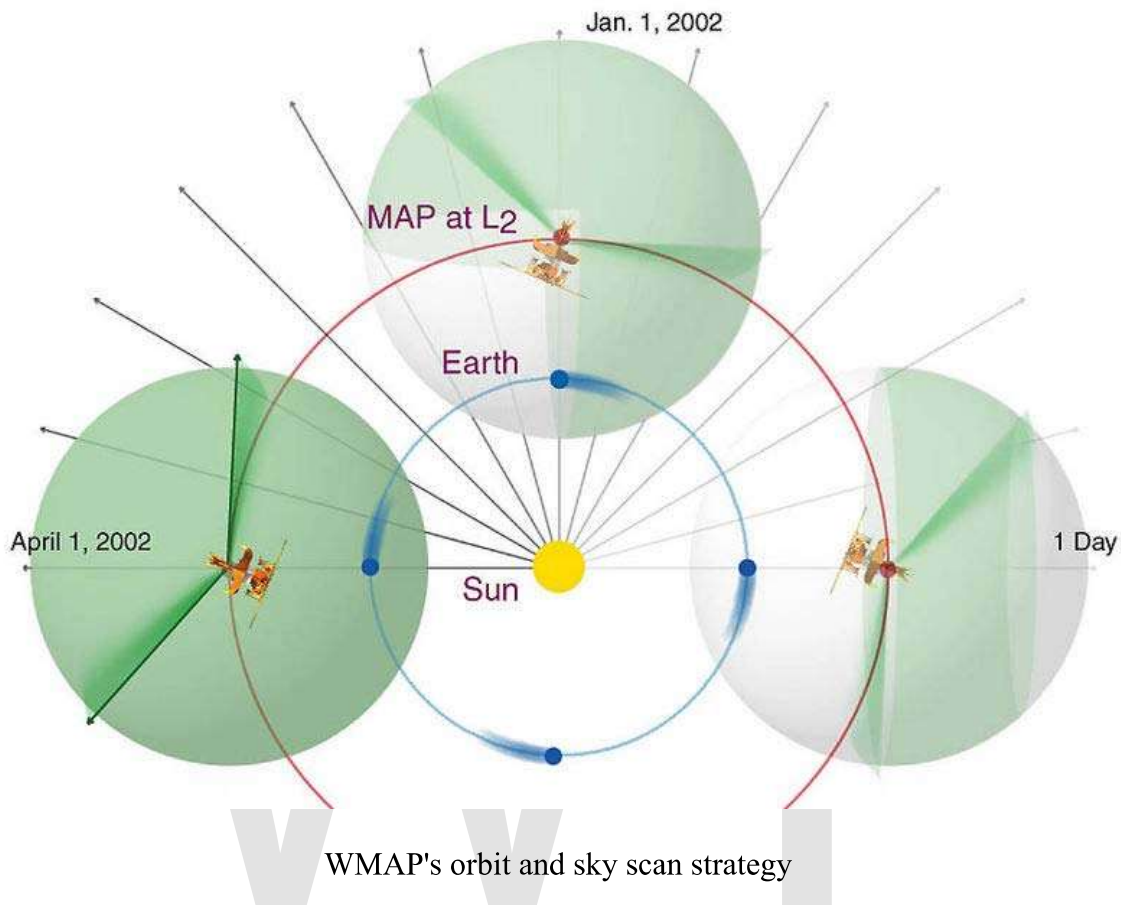


The WMAP's trajectory and orbit.



WMAP launches from Kennedy Space Center, 30 June 2001.

The WMAP spacecraft arrived at the Kennedy Space Center on 20 April 2001. After being tested for two months, it was launched via Delta II 7425 rocket on 30 June 2001. It began operating on its internal power five minutes before its launching, and so continued operating until the solar panel array deployed. The WMAP was activated and monitored while it cooled. On 2 July, it began working, first with in-flight testing (from launching until 17 August), then began constant, formal work. Afterwards, it effected three Earth-Moon phase loops, measuring its sidelobes, then flew by the Moon on 30 July, enroute to the Sun-Earth L_2 Lagrangian point, arriving there on 1 October 2001, becoming, thereby, the first CMB observation mission permanently posted there.

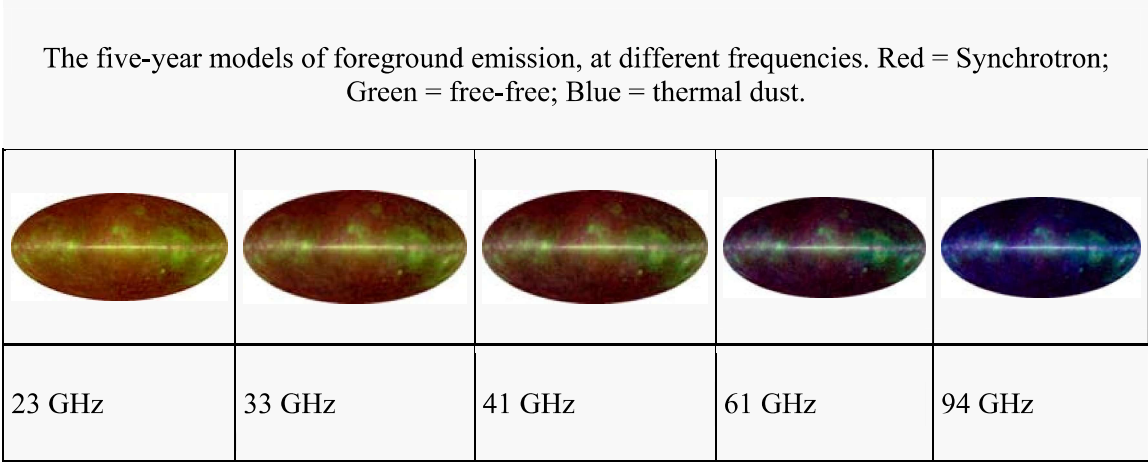


The spacecraft's location at Lagrange 2, (1.5 million kilometers from Earth) minimizes the amount of contaminating solar, terrestrial, and lunar emissions registered, and thermally stabilizes it. To view the entire sky, without looking to the sun, the WMAP traces a path around L_2 in a Lissajous orbit ca. 1.0 degree to 10 degrees, with a 6-month period. The telescope rotates once every 2 minutes, 9 seconds" (0.464 rpm) and precesses at the rate of 1 revolution per hour. WMAP measures the entire sky every six months, and completed its first, full-sky observation in April 2002.

Foreground radiation subtraction

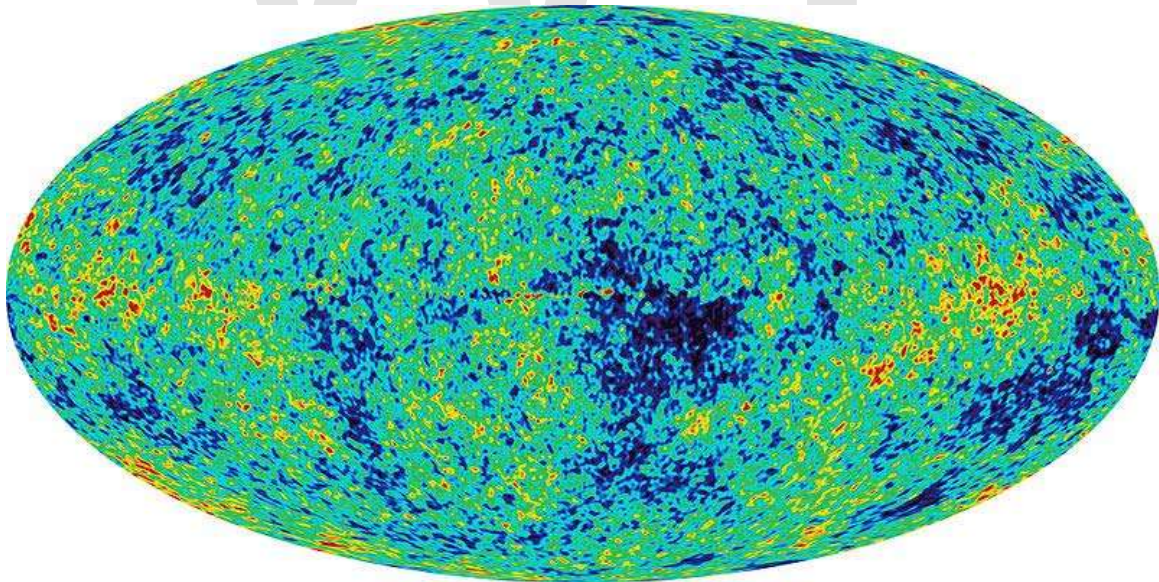
The WMAP observes in five frequencies, permitting the measurement and subtraction of foreground contamination (from the Milky Way and extra-galactic sources) of the CMB. The main emission mechanisms are synchrotron radiation and free-free emission (dominating the lower frequencies), and astrophysical dust emissions (dominating the higher frequencies). The spectral properties of these emissions contribute different amounts to the five frequencies, thus permitting their identification and subtraction.

Foreground contamination is removed in several ways. First, subtract extant emission maps from the WMAP's measurements; second, use the components' known, spectral values to identify them; third, simultaneously fit the position and spectra data of the foreground emission, using extra data sets. Foreground contamination also is reduced by using only the full-sky map portions with the least foreground contamination, whilst masking the remaining map portions.



Measurements and discoveries

One-year data release



The first-year map of the CMB.

On 11 February 2003, based upon one year's worth of WMAP data, NASA published the latest calculated age, composition, and image of the universe to date, that "contains such

stunning detail, that it may be one of the most important scientific results of recent years"; the data surpass previous CMB measurements.

Based upon the Lambda-CDM model, the WMAP team produced cosmological parameters from the WMAP's first-year results. Three sets are given below; the first and second sets are WMAP data; the difference is the addition of spectral indices, predictions of some inflationary models. The third data set combines the WMAP constraints with those from other CMB experiments (ACBAR and CBI), and constraints from the 2dF Galaxy Redshift Survey and Lyman alpha forest measurements. Note that there are degenerations among the parameters, the most significant is between n_s and τ ; the errors given are at 68% confidence.

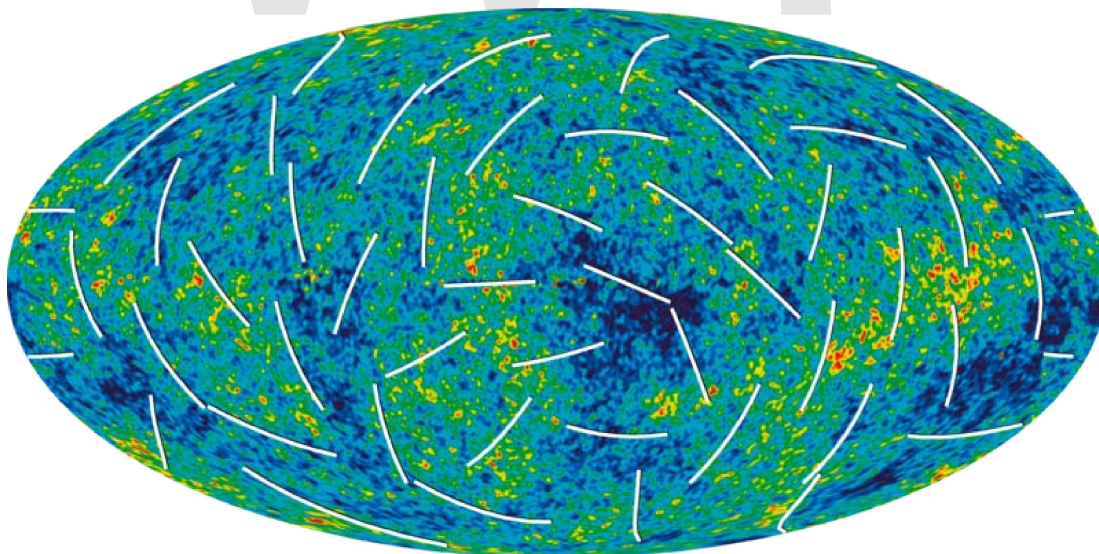
Best-fit cosmological parameters from WMAP one-year results				
Parameter	Symbol	Best fit (WMAP only)	Best fit (WMAP, extra parameter)	Best fit (all data)
Hubble's constant ($\text{km}/\text{Mpc}\cdot\text{s}$)	H_0	72 ± 5	70 ± 5	71^{+4}_{-3}
Baryonic content	$\Omega_b h^2$	0.024 ± 0.001	0.023 ± 0.002	0.0224 ± 0.0009
Matter content	$\Omega_m h^2$	0.14 ± 0.02	0.14 ± 0.02	$0.135^{+0.008}_{-0.009}$
Optical depth to reionization	τ	$0.166^{+0.076}_{-0.071}$	0.20 ± 0.07	0.17 ± 0.06
Amplitude	A	0.9 ± 0.1	0.92 ± 0.12	$0.83^{+0.09}_{-0.08}$
Scalar spectral index	n_s	0.99 ± 0.04	$0.93^{+0.07}_{-0.07}$	0.93 ± 0.03
Running of spectral index	dn_s / dk	—	-0.047 ± 0.04	$-0.031^{+0.016}_{-0.017}$

Fluctuation amplitude at $8h^{-1}$ Mpc	σ_8	0.9 ± 0.1	—	0.84 ± 0.04
Age of the universe (Ga)	t_0	13.4 ± 0.3	—	13.7 ± 0.2
Total density of the universe	Ω_{tot}	—	—	1.02 ± 0.02

Using the best-fit data and theoretical models, the WMAP team determined the times of important universal events, including the redshift of reionization, 17 ± 4 ; the redshift of decoupling, $1,089\pm 1$ (and the universe's age at decoupling, 379^{+8-7} ka); and the redshift of matter/radiation equality, $3,233^{+194-210}$. They determined the thickness of the surface of last scattering to be 195 ± 2 in redshift, or 118^{+3-2} ka. They determined the current density of baryons, $2.5\pm 0.1\times 10^{-7}$ cm^{-3} , and the ratio of baryons to photons, $6.1^{+0.3-0.2}\times 10^{-10}$. The WMAP's detection of an early reionization excluded warm dark matter.

The team also examined Milky Way emissions at the WMAP frequencies, producing a 208-point source catalogue. Also, they observed the Sunyaev-Zel'dovich effect at 2.5σ the strongest source is the Coma cluster.

Three-year data release



A map of the polarization from the 3rd year results

The three-year WMAP data were released on 17 March 2006. The data included temperature and polarization measurements of the CMB, which provided further confirmation of the standard flat Lambda-CDM model and new evidence in support of inflation.

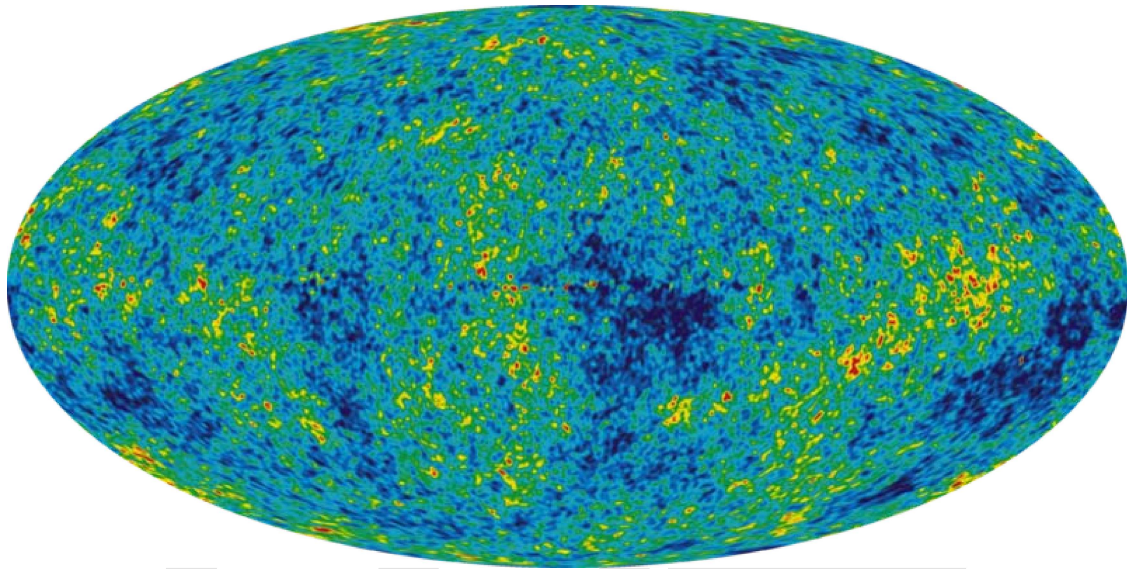
The 3-year WMAP data alone shows that the universe must have dark matter. Results were computed both only using WMAP data, and also with a mix of parameter constraints from other instruments, including other CMB experiments (ACBAR, CBI and BOOMERANG), SDSS, the 2dF Galaxy Redshift Survey, the Supernova Legacy Survey and constraints on the Hubble constant from the Hubble Space Telescope.

Best-fit cosmological parameters from WMAP three-year results		
Parameter	Symbol	Best fit (WMAP only)
Hubble's constant ($\text{km}/\text{Mpc}\cdot\text{s}$)	H_0	$73.2^{+3.1}_{-3.2}$
Baryonic content	$\Omega_b h^2$	0.0229 ± 0.00073
Matter content	$\Omega_m h^2$	$0.1277^{+0.0080}_{-0.0079}$
Optical depth to reionization ^[a]	τ	0.089 ± 0.030
Scalar spectral index	n_s	0.958 ± 0.016
Fluctuation amplitude at $8h^{-1}$ Mpc	σ_8	$0.761^{+0.049}_{-0.048}$
Age of the universe (Ga)	t_0	$13.73^{+0.16}_{-0.15}$
Tensor-to-scalar ratio ^[b]	r	< 0.65

[a] ^ Optical depth to reionization improved due to polarization measurements.

[b] ^ < 0.30 when combined with SDSS data. No indication of non-gaussianity.

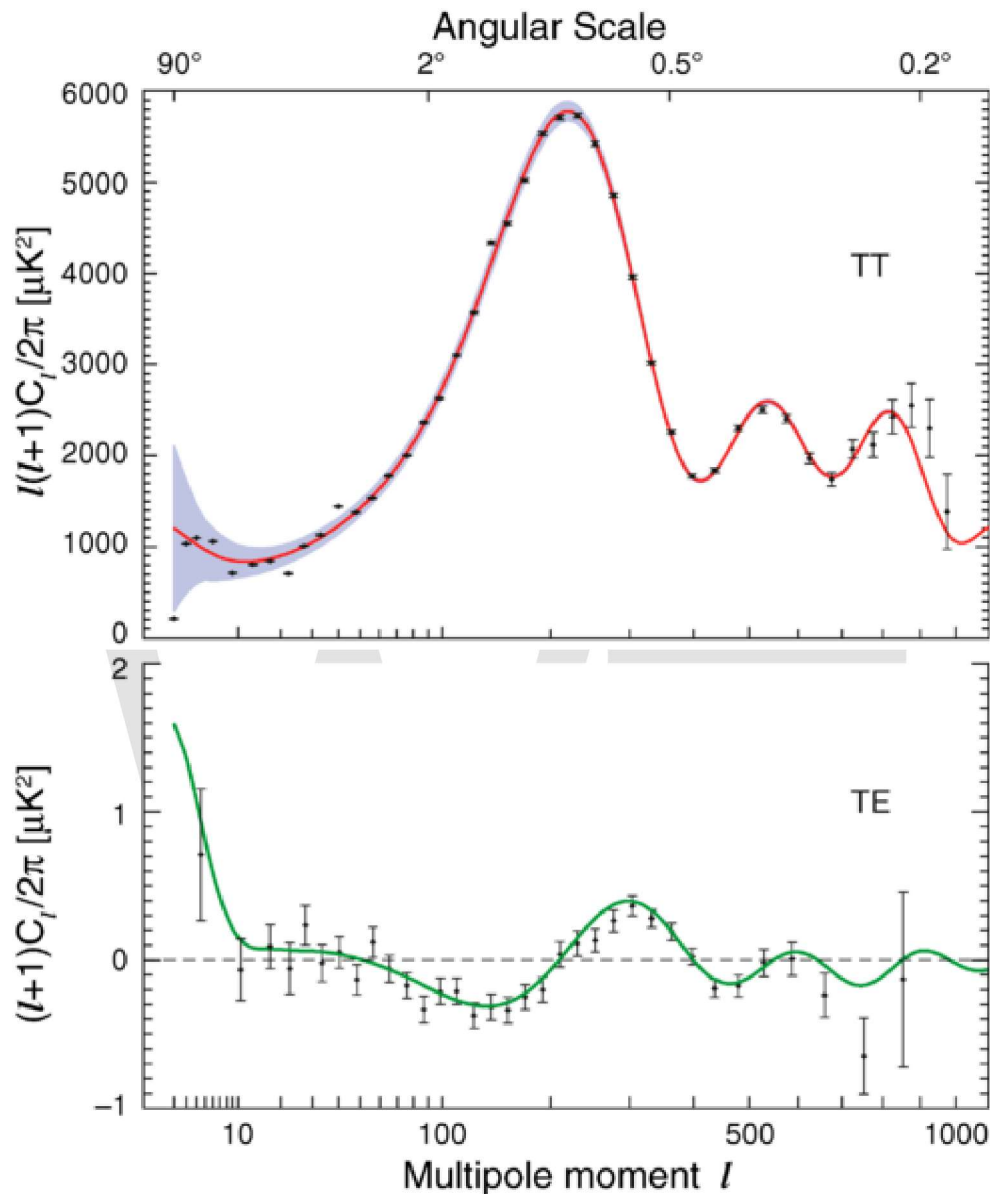
Five-year data release



5 year WMAP image of background cosmic radiation (2008)

The five-year WMAP data were released on 28 February 2008. The data included new evidence for the cosmic neutrino background, evidence that it took over half a billion years for the first stars to reionize the universe, and new constraints on cosmic inflation.

The improvement in the results came from both having an extra 2 years of measurements (the data set runs between midnight on 10 August 2001 to midnight of 9 August 2006), as well as using improved data processing techniques and a better characterization of the instrument, most notably of the beam shapes. They also make use of the 33 GHz observations for estimating cosmological parameters; previously only the 41 GHz and 61 GHz channels had been used. Finally, improved masks were used to remove foregrounds.



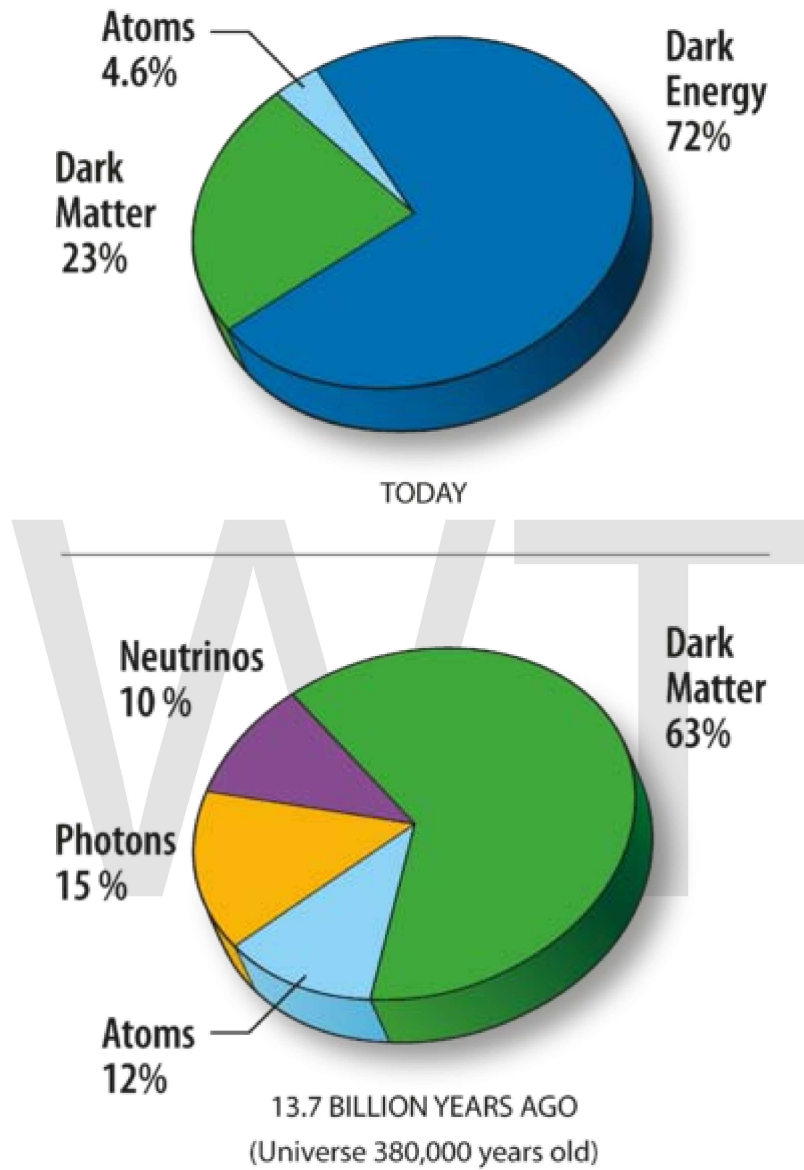
The five-year total-intensity and polarization spectra from WMAP

Improvements to the spectra were in the 3rd acoustic peak, and the polarization spectra.

The measurements put constraints on the content of the universe at the time that the CMB was emitted; at the time 10% of the universe was made up of neutrinos, 12% of atoms, 15% of photons and 63% dark matter. The contribution of dark energy at the time was negligible. It also constrained the content of the present-day universe; 4.6% atoms, 23% dark matter and 72% dark energy.

The WMAP five-year data was combined with measurements from Type Ia supernova (SNe) and Baryon acoustic oscillations (BAO).

The elliptical shape of the WMAP skymap is the result of a Mollweide projection.



Matter/energy content in the current universe (top) and at the time of photon decoupling in the recombination epoch 380,000 years after the Big Bang (bottom)

Best-fit cosmological parameters from WMAP five-year results

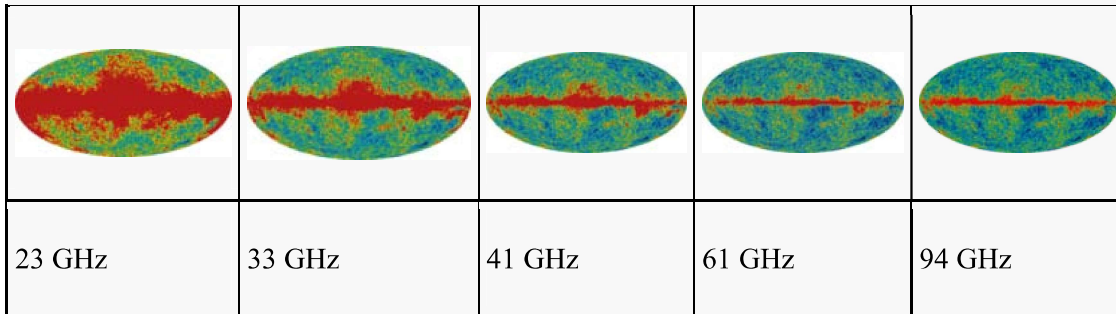
Parameter	Symbol	Best fit (WMAP only)	Best fit (WMAP + SNe + BAO)

Hubble's constant ($\text{km}/\text{Mpc}\cdot\text{s}$)	H_0	$71.9^{+2.6}_{-2.7}$	70.5 ± 1.3
Baryonic content	$\Omega_b h^2$	0.02273 ± 0.00062	$0.02267^{+0.00058}_{-0.00059}$
Cold dark matter content	$\Omega_c h^2$	0.1099 ± 0.0062	0.1131 ± 0.0034
Dark energy content	Ω_Λ	0.742 ± 0.030	0.726 ± 0.015
Optical depth to reionization	τ	0.087 ± 0.017	0.084 ± 0.016
Scalar spectral index	n_s	$0.963^{+0.014}_{-0.015}$	0.960 ± 0.013
Running of spectral index	$dn_s / d\ln k$	-0.037 ± 0.028	-0.028 ± 0.020
Fluctuation amplitude at $8h^{-1}$ Mpc	σ_8	0.796 ± 0.036	0.812 ± 0.026
Age of the universe (Ga)	t_0	13.69 ± 0.13	13.72 ± 0.12
Total density of the universe	Ω_{tot}	$1.099^{+0.100}_{-0.085}$	$1.0050^{+0.0060}_{-0.0061}$
Tensor-to-scalar ratio	r	< 0.43	< 0.22

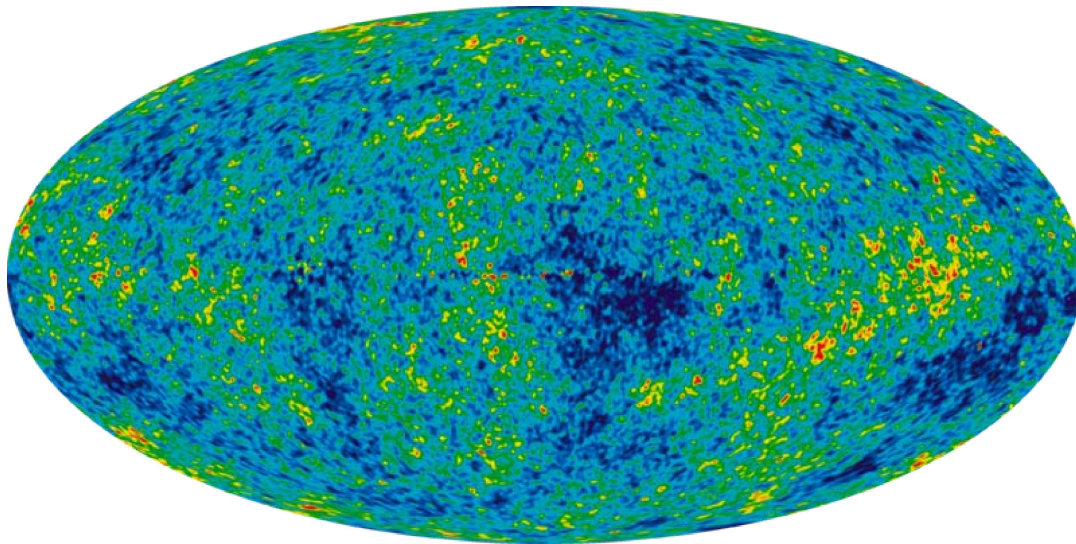
The data puts a limits on the value of the tensor-to-scalar ratio, $r < 0.22$ (95% certainty), which determines the level at which gravitational waves affect the polarization of the CMB, and also puts limits on the amount of primordial non-gaussianity. Improved constraints were put on the redshift of reionization, which is 10.9 ± 1.4 , the redshift of decoupling, $1,090.88\pm 0.72$ (as well as age of universe at decoupling, $376.971^{+3.162}_{-3.167}$ ka) and the redshift of matter/radiation equality, $3,253^{+89}_{-87}$.

The extragalactic source catalogue was expanded to include 390 sources, and variability was detected in the emission from Mars and Saturn.

The five-year maps at different frequencies from WMAP with foregrounds (the red band)



Seven-year data release



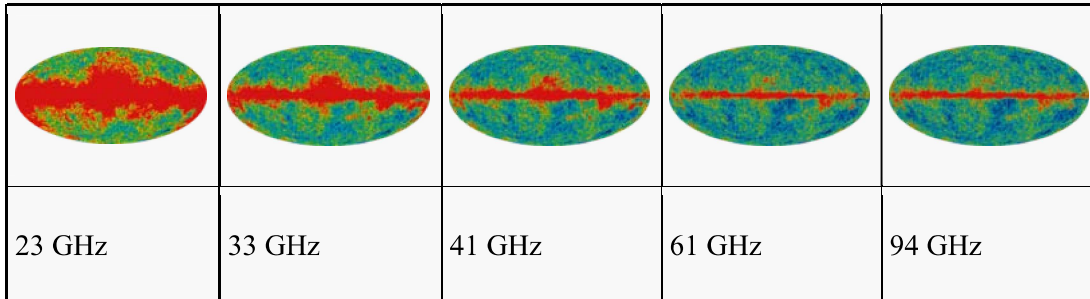
7 year WMAP image of background cosmic radiation (2010)

The Seven-year WMAP data were released on 26 January 2010. According to this data the Universe is 13.75 ± 0.11 bln. years old. As part of this release, claims for inconsistencies with the standard model were investigated. Most were shown not to be statistically significant, and likely due to *a posteriori* selection (where one sees a weird deviation, but fails to consider properly how hard one has been looking; a deviation with 1:1000 likelihood will typically be found if one tries one thousand times). For the deviations that do remain, there are no alternative cosmological ideas (for instance, there seem to be correlations with the ecliptic pole). It seems most likely these are due to other effects, with the report mentioning uncertainties in the precise beam shape and other possible small remaining instrumental and analysis issues.

The other confirmation of major significance is of the total amount of matter/energy in the Universe in the form of Dark Energy - 72.1% (within 1.5%) as non 'particle' background, and Dark Matter - 23.3% (within 1.3%) of non baryonic (sub atomic)

'particle' energy. This leaves matter, or baryonic particles (atoms) at only 4.3% (within 0.1%).

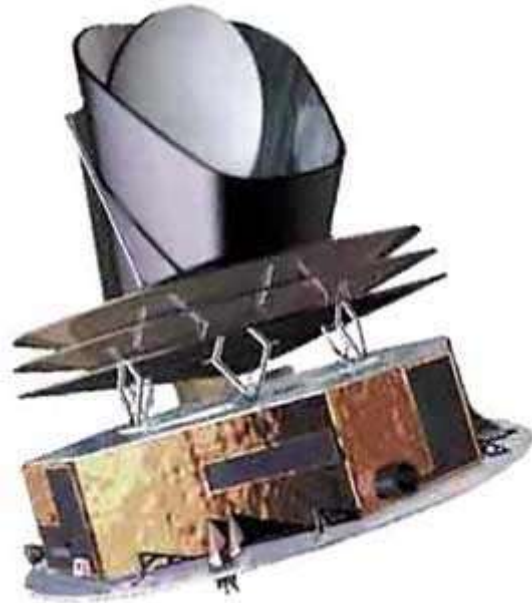
The Seven-year maps at different frequencies from WMAP with foregrounds (the red band)



Main result

The main result of the mission is contained in the various oval maps of the CMB spectrum over the years. These oval images present the temperature distribution gained by the WMAP team from the observations by the telescope of the mission. Measured is the temperature obtained from a Planck's law interpretation of the microwave background. The oval map covers the whole sky. The results describe the state of the universe only some hundred-thousand years after the "big bang", which happened roughly 13.7 billion years before our time. The microwave background is very homogeneous in temperature (the relative variations from the mean, which presently is still 2.7 Kelvins, are only of the order of 5×10^{-5}). The temperature variations corresponding to the local directions are presented through different colours (the "red" directions are hotter, the "blue" directions cooler than the average).

Future measurements



Artist's impression of the Planck spacecraft

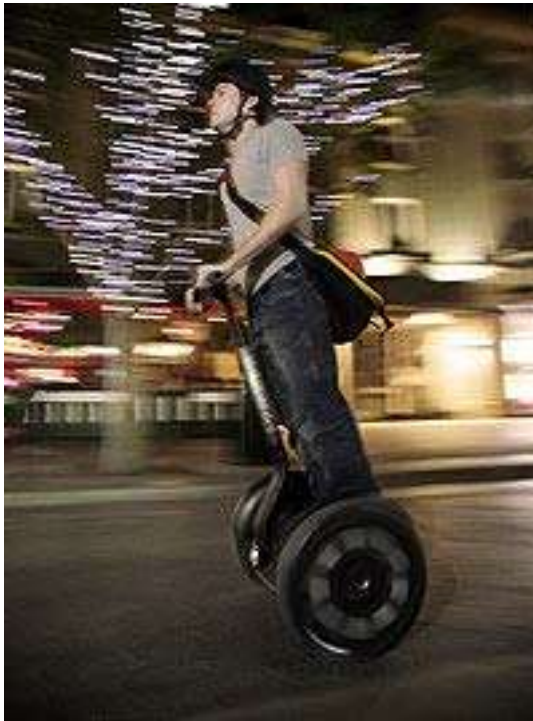
The original timeline for WMAP gave it two years of observations; these were completed by September 2003. Mission extensions were granted in both 2002 and 2004, giving the spacecraft a total of 8 observing years (the originally proposed duration), which was to end in September 2009. NASA has announced that the WMAP mission has been extended again, to September 2010, and in October 2010 the spacecraft was moved to a graveyard orbit.

WMAP's results will be built upon by several other instruments that are currently under construction. These will either be focusing on higher sensitivity total intensity measurements or measuring the polarization more accurately in the search of B-mode polarization indicative of primordial gravitational waves.

A follow-on mission is the Planck spacecraft, which launched on the 14th of May, 2009. This mission aims to measure the CMB more accurately than WMAP at all angular scales, both in total intensity and polarization. Various ground- and balloon-based instruments are being constructed to look for B-mode polarization, including EBEX.

Chapter- 2

Segway PT



Rider on Segway i2 Personal Transporter

Type	Electric vehicle
Wheels	Two
Inventor	Dean Kamen
Introduced	2001
Chief Engineer	Doug Field
	David Robinson
Dynamics Engineers	John Morrel
	Jon Stevens
	Jon Pompa

Programmers
Chuck Herscovici
Gerry Rigdon
Michael Kaufman
Eric Pribyl
Jim Dattalo

Electrical Engineers
Phil Lemay
Mike Gansler
JD Heinzmann
Jason Sachs
Larry Liberman
Chris Kastel
Zeta Electronics

Mechanical Engineers
Ron Reich
Ray Debruin
Mike Slate
JR Holt

Industrial Designers
Scott Water
Tao Chang

The **Segway PT** is a two-wheeled, self-balancing electric vehicle invented by Dean Kamen. It is produced by Segway Inc. of New Hampshire, USA. The name "Segway" is a homophone of "segue" (a smooth transition, literally Italian for "follows") while "PT" denotes personal transporter.

Computers and motors in the base of the device keep the Segway PT upright when powered on with balancing enabled. Users lean forward to go forward, lean back to go backward, and turn by using a "Lean Steer" handlebar, leaning it left or right. Segway PTs are driven by electric motors at up to 12.5 miles per hour (20.1 km/h). gyroscopic sensors are used to detect tilting of the device which indicates a departure from perfect balance. Motors driving the wheels are commanded as needed to bring the PT back into balance.



W V I



Technology



The Segway PT's detachable wireless InfoKey

The dynamics of the Segway PT are identical to a classic control problem, the inverted pendulum. The Segway PT (*PT* is an initialism for *personal transporter* while the old suffix *HT* was an initialism for *human transporter*) has electric motors powered by Valence Technology phosphate-based lithium-ion batteries which can be charged from household current. It balances with the help of dual computers running proprietary software, two tilt sensors, and five gyroscopic sensors. The servo drive motors rotate the wheels forwards or backwards as needed for balance or propulsion. The rider changes acceleration by leaning forward or backwards in the direction he or she wishes to travel. On older models, steering is controlled by a twist grip on the left handlebar, which simply varies the speeds between the two motors, rotating the Segway PT (a decrease in the speed of the left wheel would turn the Segway PT to the left). Newer models enable the use of "leaning" to steer as well as move forwards or backwards.



WV I







The Segway PT is built to stay balanced in one place. Designed to mirror the process of human walking, if the rider standing on an initially balanced Segway PT leans forward, therefore upsetting the balance, the PT moves forward to regain balance just as in walking a leg moves forward to retain balance. With the Segway PT, changes from a balanced status are first detected by the gyro sensors, and signals are passed on to the onboard computers which then direct motors to regain balance. This process occurs about 100 times per second, so small adjustments to maintain balance occur almost immediately after the balance is upset by the rider.

The side effect of this balancing system is that as the Segway PT balances itself the entire unit changes position in the direction it has moved to restore balance. (For example, if the rider leans forward, the entire Segway PT will move forward from its original position, until the rider restores an upright position on the unit.) This is precisely how the Segway PT is controlled - the balancing and movement is essentially one combined system.

The Segway PT features a governor (speed limiting) mechanism. When the Segway PT approaches the maximum speed allowed by the software, it intentionally begins to tilt slightly backwards. This moves the platform out in front, and leans the handlebars backwards towards the rider, eventually nudging the rider to lean back slightly and slow the Segway PT down. If not for the governor, riders would be able to lean farther than the motor could ever compensate for. The Segway PT also slows or stops immediately if the handlebar of the unit (or forward bag) nudges into any obstacle.

Uses





Two tourists on a Segway tour in Florence, Italy.

Segways perform best in areas with adequate sidewalks, curb cuts at intersections, and ramps. They are used in some theme parks by visitors and employees. Angel Island State Park, in San Francisco Bay in California, offers Segway tours, but prohibits personal Segways except as needed by disabled visitors. The special police forces trained to protect the public during the 2008 Summer Olympics used the Segway for mobility.











Though a Segway-focused organization, Disability Rights Advocates for Technology, advocates for Segway PT sidewalk and facility access as an ADA issue, Segways cannot be marketed in the US as medical devices: they have not been approved by the Food and Drug Administration as a medical device and Johnson & Johnson claims exclusive rights to the medical uses of the balancing technology found in the iBOT and Segway. Dean Kamen sold the medical rights to the technology of the iBOT, a very stable and mobile powered wheelchair, to Johnson & Johnson.

A version of the Segway i2 is being marketed to the Emergency Medical Services community. Equipped with light bars and a variety of hard and soft cases, it is sealed against wet conditions, and rated for 24 miles (38.6 km) per charge.





WV I







Restrictions on use

North America

- Canada: Restrictions on motorized vehicle use are set by provinces individually. In Alberta, Segways cannot be driven on Public Roads including sidewalks abutting public roads. Segways cannot be driven on city-owned bicycle paths in Calgary. Segways are allowed to be driven on private land with the landowner's permission. (Some malls allow their use.) In British Columbia, Segways can't legally be operated on B.C. roads or on sidewalks because they cannot be licensed or insured as a vehicle in B.C.



Guided Segway tour in Washington, D.C.

- United States, general: The company has challenged bans and sought exemption from pavement restrictions in over 30 states. The Segway PT has been banned from use on sidewalks and in public transportation in a few municipalities, often because it is not classified as a medical device. Advocacy groups for pedestrians and the blind in the US have been critical of Segway PT use: America Walks and the American Council of the Blind oppose allowing the PT to be driven on sidewalks, even for those with disabilities, and have actively lobbied against any such legislation. Today, Segways are allowed to be used on sidewalks in most states, although local municipalities may disallow their use. Many states also allow their use in bicycle lanes or on roads with speed limits of up to 25 mph.
- United States, San Francisco: In November 2002, before it was widely available, the city of San Francisco banned the Segway PT from sidewalks citing safety concerns. However, a number of Segway Tour operations use them in cycle lanes and designated trails.
- United States, Disney: In February 2004, Disney banned Segway PTs from its theme parks, stating they had not been approved by the FDA as medical devices. In the same month, Disney began offering Segway tours of its Epcot theme park. In early August 2007, Disney began offering a similar guided tour in its Disney's California Adventure park in California.
- Mexico: In Mexico there is not a regulation that limits their use in public spaces.

Asia

- Japan: the Segway is treated as a motorcycle with an engine displacement between 50 cc and 125 cc. As such, the vehicle must be equipped with brakes and signal lights, and must register for a license plate, making it virtually impossible to lawfully use a Segway on public roads.

Middle East

- Israel: as of 2006 Segways may be used on sidewalks and all other pedestrian designated locations, as well as on roads that either have no sidewalks, have obstructed sidewalks or have sidewalks lacking curb cuts. The user must be over 16 years old and does not require a license. The maximum allowed speed is 13 km/h (8.1 mph), enforced by electronic restriction put in place by the importer, who in turn must do so in order to obtain the import license for the vehicle.

WWT

Europe



Segway in Germany. Red light and license plate are equipped.

Segways are used in Europe, but mainly in niche markets (such as guided city tours); they are not commonly used as a means of transportation. Their use on public streets is allowed in most countries, but often with various restrictions. Most countries also require vehicle insurance and a license plate.

- Austria: In Vienna, Segways can be rented in the Prater amusement park; a Segway dealer in central Vienna also offers Segways for rent.

- Czech Republic: the use of a Segway is allowed wherever pedestrians and bicycles are allowed. Segways can be rented for city tours, for example on the Old Town Square, Prague.
- Denmark: the Segway is classified as a moped (*knallert*). As such vehicles are required to be fitted with lights, license plates and mechanical brakes, the Segway is effectively banned from public roads. Recently, a trial where the segway would be classified as a bicycle has been announced running from 1 June 2010 to 1 April 2011
- Germany: the use of a Segway PT i2 is generally allowed on bicycle paths and public roads within city limits since 25 July 2009. Outside city limits, the Segway may not be used on federal motorways, federal highways, state roads, and district roads. Bicycle lanes must be used if present. Riding a Segway on sidewalks and in pedestrian zones for city tours requires a special permit. The Segway is classified as an "electronic mobility aid", a new class of vehicle defined specifically for the Segway PT. Segways used on public roads must be equipped with front and rear lighting, reflectors, a bell, and an insurance indicator plate. The driver must have procured a vehicle insurance and hold at least an *M type* (moped) license.
- Italy: the use of the Segway is allowed within city limits wherever pedestrian and bicycles are allowed, i.e., sidewalks, bicycle paths, parks, etc.
- Netherlands: In April 2008, the Dutch Government announced that it would ease the ban it had imposed in January 2007 that made it illegal to use a Segway on public roads in the Netherlands. Until recently, a tolerance policy was in place due to the inability of the authorities to classify the Segway as a vehicle. However, certain handicapped people, primarily heart and lung patients, are allowed to use the Segway, but only on the pavement. From 1 July 2008, anyone over the age of 16 is permitted to use a Segway on Dutch roads but users need to buy custom insurance. Amsterdam police officers are testing the Segway. In Rotterdam the Segway is used regularly by police officers and city watches.
- Portugal: Segways are legal on public paths from age 18 (and below, when accompanied by adults) as an equivalent to pedestrian traffic and are used by many local police forces (*Policia Municipal*), and by *Policia Maritima* (a Navy unit), for beach patrolling. They are also used (rented) by tour operators across the country.
- Sweden: It was unlawful to use a Segway on any public road or pavement in Sweden until 18 December 2008 when the Segway was re-classified as a *cykel klass II* (class 2 bicycle).
- Switzerland: the Segway is classified as a light motorcycle. Only the PT i2 has been approved for use in Switzerland. The PT i2 may be used on roads provided that it is equipped with a Swiss Road Kit and a license plate. The Swiss Road Kit

has front and back lighting, a battery source, and a license plate holder. Use on sidewalks and pedestrian zones is prohibited. An exception is made for handicapped individuals who must obtain in advance a special authorization from the Swiss Federal Roads Office. The Segway PT i180 may also be registered for use on specific request. However, the PT i180 must be equipped with a left/right turn indicator system before it may be admitted for road use.

- United Kingdom: in UK the Segway is classified as a powered vehicle and subject to Road Traffic law, with the effect that because the Segway is deemed not to meet the required safety standards it is unlawful to use a Segway anywhere other than on private property with the owner's permission. While in opposition, the political parties forming the current coalition government, the Conservatives and Liberal Democrats, lobbied the then Government to change the law to allow Segways to use public cycle lanes. In July 2010, a man was charged under the Highways Act 1835 in Barnsley for riding his Segway on the pavement, which led to him being prosecuted and fined £75 in January 2011.

Oceania

- Australia: laws are determined at the state level, each differing in their adoption of the Australian Road Rules. In New South Wales, the Segway has been confirmed by the Roads and Traffic Authority as being illegal on both roads and footpaths. "In simple terms, riders are way too exposed to mix with general traffic on a road and too fast, heavy and consequently dangerous to other users on footpaths or cycle paths." Although this does not render them totally illegal (they may still, for example, be used on private property), their uses are limited enough that they are not sold to the general public.
- New Zealand: The Segway PT is classed as a Mobility Device, in the same category as a mobility scooter or electric wheelchair. Mobility Devices must be ridden on footpaths where possible, at a speed that does not endanger others, and give way to pedestrians.

Chapter- 3

SERF

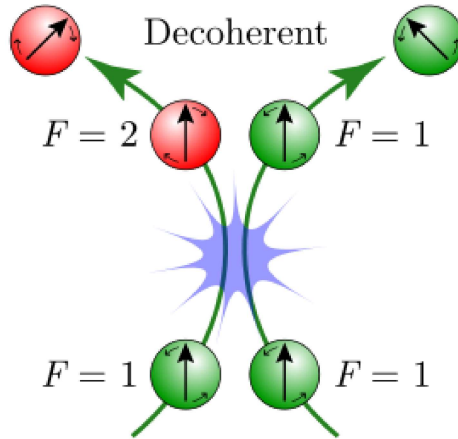
A **spin exchange relaxation-free (SERF) magnetometer** is a type of magnetometer developed at Princeton University in the early 2000s. SERF magnetometers measure magnetic fields by using lasers to detect the interaction between alkali metal atoms in a vapor and the magnetic field.

The name for the technique comes from the fact that spin exchange relaxation, a mechanism which usually scrambles the orientation of atomic spins, is avoided in these magnetometers. This is done by using a high (10^{14} cm^{-3}) density of Potassium atoms and a very low magnetic field. Under these conditions, the atoms exchange spin quickly compared to their magnetic precession frequency so that the average spin interacts with the field and is not destroyed by decoherence.

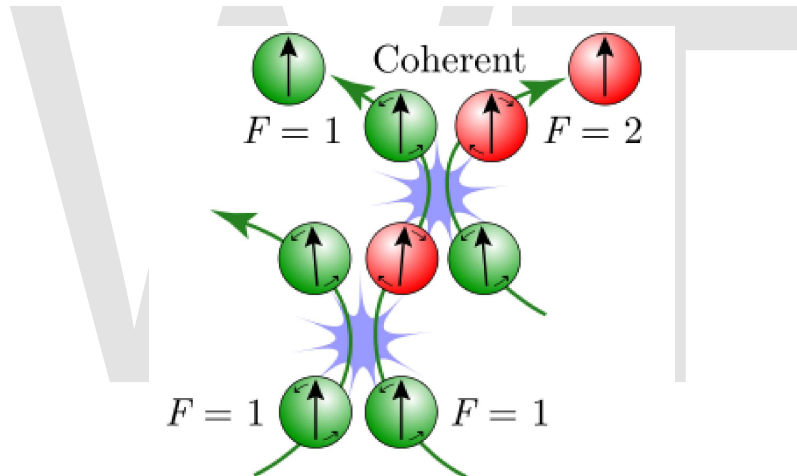
A spin-exchange relaxation-free (SERF) magnetometer achieves very high magnetic field sensitivity by monitoring a high density vapor of alkali metal atoms precessing in a near-zero magnetic field. The sensitivity of SERF magnetometers improves upon traditional atomic magnetometers by eliminating the dominant cause of atomic spin decoherence caused by spin-exchange collisions among the alkali metal atoms. SERF magnetometers are among the most sensitive magnetic field sensors and in some cases exceed the performance of SQUID detectors of equivalent size. A small 1 cm^3 volume glass cell containing potassium vapor has reported $1 \text{ fT}/\sqrt{\text{Hz}}$ sensitivity and can theoretically become even more sensitive with larger volumes. They are vector magnetometers capable of measuring all three components of the magnetic field simultaneously.

Spin-exchange relaxation

Spin-exchange collisions preserve total angular momentum of a colliding pair of atoms but can scramble the hyperfine state of the atoms. Atoms in different hyperfine states do not precess coherently and thereby limit the coherence lifetime of the atoms. However, decoherence due to spin-exchange collisions can be nearly eliminated if the spin-exchange collisions occur much faster than the precession frequency of the atoms. In this regime of fast spin-exchange, all atoms in an ensemble rapidly change hyperfine states, spending the same amounts of time in each hyperfine state and causing the spin ensemble to precess more slowly but remain coherent. This so-called SERF regime can be reached by operating with sufficiently high alkali metal density (at higher temperature) and in sufficiently low magnetic field.



Alkali metal atoms with hyperfine state indicated by color precessing in the presence of a magnetic field experience a spin-exchange collision which preserves total angular momentum but changes the hyperfine state, causing the atoms to precess in opposite directions and decohere.



Alkali metal atoms in the spin-exchange relaxation-free (SERF) regime with hyperfine state indicated by color precessing in the presence of a magnetic field experience two spin-exchange collisions in rapid succession which preserves total angular momentum but changes the hyperfine state, causing the atoms to precess in opposite directions only slightly before a second spin-exchange collision returns the atoms to the original hyperfine state.

The spin-exchange relaxation rate R_{se} for atoms with low polarization experiencing slow spin-exchange can be expressed as follows:

$$R_{se} = \frac{1}{2\pi T_{se}} \left(\frac{2I(2I-1)}{3(2I+1)^2} \right)$$

where T_{se} is the time between spin-exchange collisions, I is the nuclear spin, ν is the magnetic resonance frequency, γ_e is the gyromagnetic ratio for an electron.

In the limit of fast spin-exchange and small magnetic field, the spin-exchange relaxation rate vanishes for sufficiently small magnetic field:

$$R_{se} = \frac{\gamma_e^2 B^2 T_{se}}{2\pi} \frac{1}{2} \left(1 - \frac{(2I + 1)^2}{Q^2} \right)$$

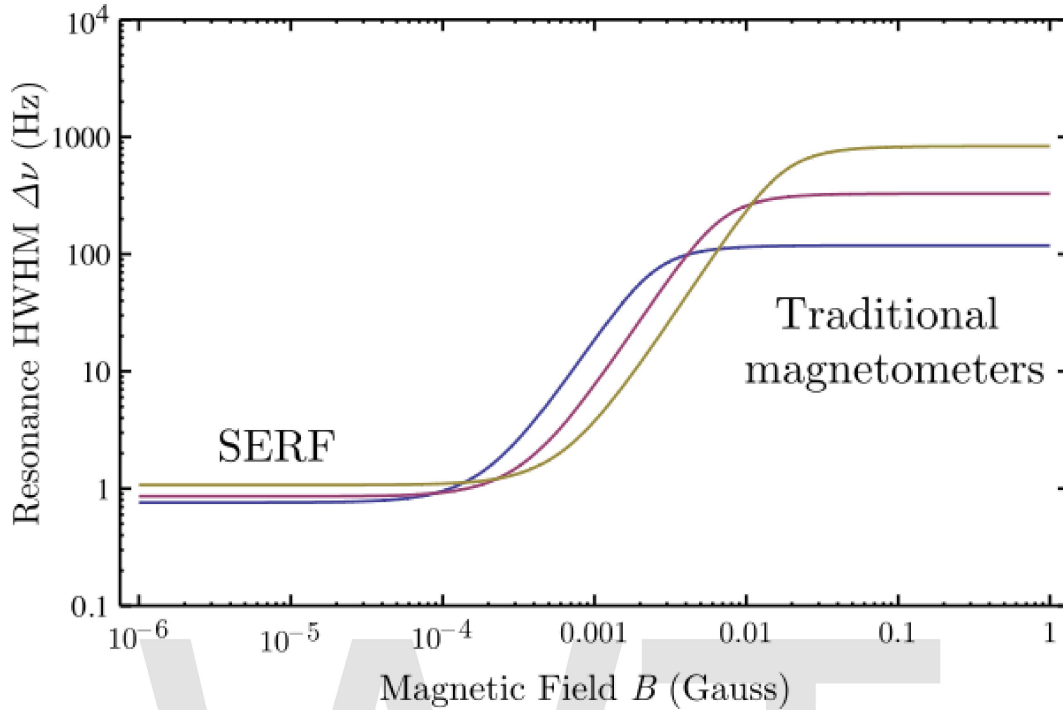
where Q is the "slowing-down" constant to account for sharing of angular momentum between the electron and nuclear spins:

$$Q(I = 3/2) = 4 \left(2 - \frac{4}{3 + P^2} \right)^{-1}$$

$$Q(I = 5/2) = 6 \left(3 - \frac{48(1 + P^2)}{19 + 26P^2 + 3P^4} \right)^{-1}$$

$$Q(I = 7/2) = 8 \left(\frac{4(1 + 7P^2 + 7P^4 + P^6)}{11 + 35P^2 + 17P^4 + P^6} \right)^{-1}$$

where P is the average polarization of the atoms. The atoms suffering fast spin-exchange precess more slowly when they are not fully polarized because they spend a fraction of the time in different hyperfine states precessing at different frequencies (or in the opposite direction).



Relaxation rate $R_{tot} = Q\Delta\nu$ as indicated by magnetic resonance linewidth for atoms as a function of magnetic field. These lines represent operation with K vapor at 160, 180 and 200 C (higher temperature provides higher relaxation rate here). using a 2 cm diameter cell with 3 atm He buffer gas, 60 Torr N₂ quenching gas. The SERF regime is clearly apparent for sufficiently low magnetic fields where the spin-exchange collisions occur much faster than the spin precession.

Sensitivity

The sensitivity δB of atomic magnetometers are limited by the number of atoms N and their spin coherence lifetime T_2 according to

$$\delta B = \frac{1}{\gamma} \sqrt{\frac{2R_{tot}Q}{F_z N}}$$

where γ is the gyromagnetic ratio of the atom and F_z is the average polarization of total atomic spin $F = I + S$.

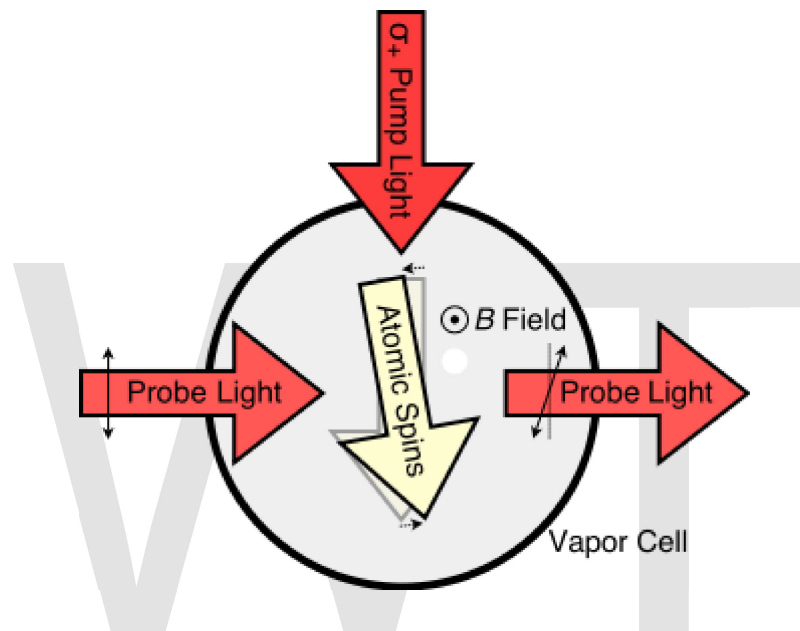
In the absence of spin-exchange relaxation, a variety of other relaxation mechanisms contribute to the decoherence of atomic spin:

$$R_{tot} = R_D + R_{sd,self} + R_{sd,He} + R_{sd,N_2}$$

where R_D is the relaxation rate due to collisions with the cell walls and $R_{sd,X}$ are the spin destruction rates for collisions among the alkali metal atoms and collisions between alkali atoms and any other gasses that may be present.

In an optimal configuration, a density of 10^{14} cm^{-3} potassium atoms in a 1 cm^3 vapor cell with $\sim 3 \text{ atm}$ helium buffer gas can achieve $10 \text{ aT Hz}^{-1/2}$ ($10^{-17} \text{ T Hz}^{-1/2}$) sensitivity with relaxation rate $R_{tot} \approx 1 \text{ Hz}$.

Typical operation



Atomic magnetometer principle of operation, depicting alkali atoms polarized by a circularly polarized pump beam, precessing in the presence of a magnetic field and being detected by optical rotation of a linearly polarized probe beam.

Alkali metal vapor of sufficient density is obtained by simply heating solid alkali metal inside the vapor cell. A typical SERF atomic magnetometer can take advantage of low noise diode lasers to polarize and monitor spin precession. Circularly polarized pumping light tuned to the D_1 spectral resonance line polarizes the atoms. An orthogonal probe beam detects the precession using optical rotation of linearly polarized light. In a typical SERF magnetometer, the spins merely tip by a very small angle because the precession frequency is slow compared to the relaxation rates.

Advantages and disadvantages

SERF magnetometers compete with SQUID magnetometers for use in a variety of applications. The SERF magnetometer has the following advantages:

- Equal or better sensitivity per unit volume
- Cryogen-free operation

- All-optical measurement limits enables imaging and eliminates interference.

Potential disadvantages:

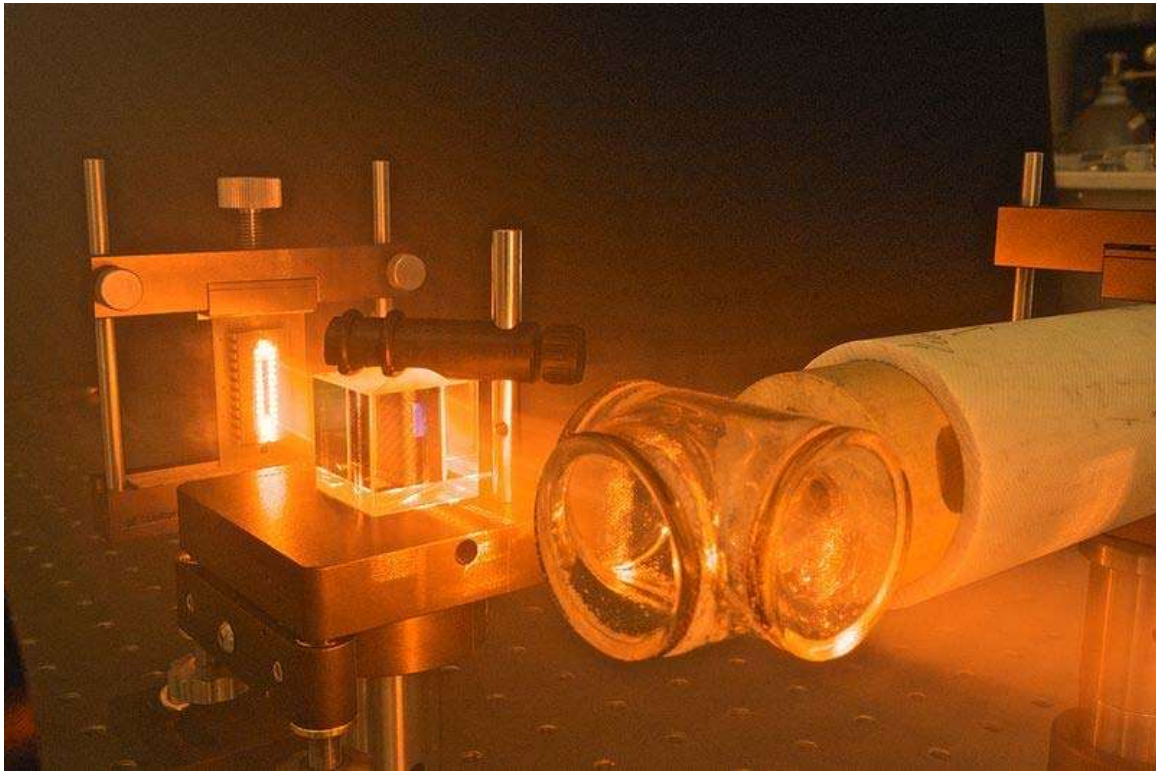
- Can only operate near zero field.
- Sensor vapor cell must be heated.

Applications

Applications utilizing high sensitivity of SERF magnetometers potentially include:

- High-performance magnetoencephalographic imaging.
- Sample magnetization measurement, especially rock samples.

History



SERF components mockup.

The SERF magnetometer was developed by Michael V. Romalis at Princeton University in the early 2000s. The underlying physics governing the suppression spin-exchange relaxation was developed decades earlier by William Happer but the application to magnetic field measurement was not explored at that time. The name "SERF" was partially motivated by its relationship to SQUID detectors in a marine metaphor.

Chapter- 4

Fermionic Condensate

A **fermionic condensate** is a superfluid phase formed by fermionic particles at low temperatures. It is closely related to the Bose–Einstein condensate, a superfluid phase formed by bosonic atoms under similar conditions. Unlike the Bose–Einstein condensates, fermionic condensates are formed using fermions instead of bosons. The earliest recognized fermionic condensate described the state of electrons in a superconductor; the physics of other examples including recent work with fermionic atoms is analogous. The first atomic fermionic condensate was created by Deborah S. Jin in 2003. A **chiral condensate** is an example of a fermionic condensate that appears in theories of massless fermions with chiral symmetry breaking.

Background

Superfluidity

Fermionic condensates are called the sixth state of matter. They are attained at temperatures lower than Bose–Einstein condensates. Fermionic condensates are a type of superfluid. As the name suggests, a superfluid possesses fluid properties similar to those possessed by ordinary liquids and gases, such as the lack of a definite shape and the ability to flow in response to applied forces. However, superfluids possess some properties that do not appear in ordinary matter. For instance, they can flow at low velocities without dissipating any energy—i.e. zero viscosity. At higher velocities, energy is dissipated by the formation of quantized vortices, which act as "holes" in the medium where superfluidity breaks down.

Superfluidity was originally discovered in liquid helium-4, in 1938, by Pyotr Kapitsa, John Allen and Don Misener. Superfluidity in helium-4, which occurs at temperatures below 2.17 kelvins (K), has long been understood to result from Bose condensation, the same mechanism that produces the Bose–Einstein condensates. The primary difference between superfluid helium and a Bose–Einstein condensate is that the former is condensed from a liquid while the latter is condensed from a gas.

Fermionic superfluids

It is far more difficult to produce a fermionic superfluid than a bosonic one, because the Pauli exclusion principle prohibits fermions from occupying the same quantum state. However, there is a well-known mechanism by which a superfluid may be formed from fermions. This is the BCS transition, discovered in 1957 by John Bardeen, Leon Cooper and Robert Schrieffer for describing superconductivity. These authors showed that, below a certain temperature, electrons (which are fermions) can pair up to form bound pairs now known as Cooper pairs. As long as collisions with the ionic lattice of the solid do not supply enough energy to break the Cooper pairs, the electron fluid will be able to flow without dissipation. As a result, it becomes a superfluid, and the material through which it flows a superconductor.

The BCS theory was phenomenally successful in describing superconductors. Soon after the publication of the BCS paper, several theorists proposed that a similar phenomenon could occur in fluids made up of fermions other than electrons, such as helium-3 atoms. These speculations were confirmed in 1971, when experiments performed by Douglas D. Osheroff showed that helium-3 becomes a superfluid below 0.0025 K. It was soon verified that the superfluidity of helium-3 arises from a BCS-like mechanism. (The theory of superfluid helium-3 is a little more complicated than the BCS theory of superconductivity. These complications arise because helium atoms repel each other much more strongly than electrons, but the basic idea is the same.)

Creation of the first fermionic condensates

When Eric Cornell and Carl Wieman produced a Bose–Einstein condensate from rubidium atoms in 1995, there naturally arose the prospect of creating a similar sort of condensate made from fermionic atoms, which would form a superfluid by the BCS mechanism. However, early calculations indicated that the temperature required for producing Cooper pairing in atoms would be too cold to achieve. In 2001, Murray Holland at JILA suggested a way of bypassing this difficulty. He speculated that fermionic atoms could be coaxed into pairing up by subjecting them to a strong magnetic field.

In 2003, working on Holland's suggestion, Deborah Jin at JILA, Rudolf Grimm at the University of Innsbruck, and Wolfgang Ketterle at MIT managed to coax fermionic atoms into forming molecular bosons, which then underwent Bose–Einstein condensation. However, this was not a true fermionic condensate. On December 16th of the same year, Jin managed to produce a condensate out of fermionic atoms for the first time. The experiment involved 500,000 potassium-40 atoms cooled to a temperature of 5×10^{-8} K, subjected to a time-varying magnetic field. The findings were published in the online edition of *Physical Review Letters* on January 24, 2004.

Examples

BCS theory

The BCS theory of superconductivity has a fermion condensate. A pair of electrons in a metal, with opposite spins can form a scalar bound state called a Cooper pair. Then, the bound states themselves form a condensate. Since the Cooper pair has electric charge, this fermion condensate breaks the electromagnetic gauge symmetry of a superconductor, giving rise to the wonderful electromagnetic properties of such states.

QCD

In quantum chromodynamics (QCD) the chiral condensate is also called the **quark condensate**. This property of the QCD vacuum is partly responsible for giving masses to hadrons (along with other condensates like the gluon condensate).

In an approximate version of QCD, which has vanishing quark masses for N quark flavours, there is an exact chiral $SU(N) \times SU(N)$ symmetry of the theory. The QCD vacuum breaks this symmetry to $SU(N)$ by forming a quark condensate. The quark condensate is therefore an order parameter of transitions between several phases of quark matter in this limit.

This is very similar to the BCS theory of superconductivity. The Cooper pairs are analogous to the pseudoscalar mesons. However, the vacuum carries no charge. Hence all the gauge symmetries are unbroken. Corrections for the masses of the quarks can be incorporated using chiral perturbation theory.

Helium-3 superfluid

A helium-3 atom is a fermion and at very low temperatures, they form two-atom Cooper pairs which are bosonic and condense into a superfluid. These Cooper pairs are substantially larger than the interatomic separation

Chapter- 5

HPV Vaccine

The human papillomavirus (HPV) vaccine is a vaccine that prevents infection with certain species of human papillomavirus associated with the development of cervical cancer and genital warts. In work that was initiated in the mid 1980s, the vaccine was co-developed, in parallel, by Dr. Richard Reichman, Dr. William Bonnez, and Dr. Robert Rose at Georgetown University Medical Center, the University of Rochester, and the National Cancer Institute.

The **human papillomavirus (HPV) vaccine** may prevent infection with certain species of human papillomavirus associated with the development of cervical cancer, genital warts, and some less common cancers. Two HPV vaccines are currently on the market: Gardasil and Cervarix. Both vaccines protect against the two HPV types (HPV-16 and HPV-18) that cause 70% of cervical cancers, and cause some other genital cancers; Gardasil also protects against the two HPV types (HPV-6 and HPV-11) that cause 90% of genital warts. In addition, Gardasil has been shown to prevent potential precursors to anal, vulvar, vaginal, and penile cancers. HPV vaccines are expected to protect against HPV induced cancers of these areas as well as HPV induced oral cancers.

Public health officials in Australia, Canada, Europe, and the United States recommend vaccination of young women against HPV to prevent cervical cancer, and to reduce the number of painful and costly treatments for cervical intraepithelial neoplasia, which is caused by HPV.

Worldwide, HPV is the most common sexually transmitted infection in adults. For example, more than 80% of American women will have contracted at least one strain of HPV by age fifty.

Although most women infected with genital HPV will not have complications from the virus, worldwide there are an estimated 470,000 new cases of cervical cancer that result in 233,000 deaths per year. About eighty percent of deaths from cervical cancer occur in poor countries. In the United States, most of the approximately 11,000 cervical cancers found annually occur in women who have never had a Pap smear, or not had one in the previous five years. HPV is also the cause of cervical intraepithelial neoplasia (CIN). CIN is a precursor to cervical cancer, and is painful and costly to treat. It is not known how many women worldwide are diagnosed with CIN.

Since the vaccine only covers some high-risk types of HPV, experts still recommend regular Pap smear screening even after vaccination.

Gardasil has been shown to also be effective in preventing genital warts in males, and use for men and boys was approved by the U.S. Food and Drug Administration (FDA) on October 16, 2009.

Efficacy

Both Gardasil and Cervarix have been shown to prevent cervical dysplasia from the HPV strains that they target, that is, types 16, 18, 6, and 11 for Gardasil and types 16 and 18 for Cervarix. This effect has lasted 4 years after vaccination for Gardasil and more than 6 years for Cervarix. As of September 2010, it is thought that booster vaccines will not be necessary.

The vaccines also offer some protection against a few high-risk HPV types that are closely related to HPVs 16 and 18. Cervarix has been shown to offer some protection against types 45 and 31, similarly, Gardasil has been shown to offer some protection against type 31, and 9 others. However, there are other high-risk HPV types are not affected by the vaccines.

Safety

Gardasil is a 3-dose (injection) vaccine. As of 1 September 2009 there have been more than 26 million doses distributed in the United States, and there have been 15,037 Vaccine Adverse Event Reporting System (VAERS) reports following the vaccination. Ninety-three percent were reports of events considered to be non-serious (e.g., fainting, pain and swelling at the injection site (arm), headache, nausea and fever), and seven percent were considered to be serious (death, permanent disability, life-threatening illness and hospitalization). There is no proven causal link between the vaccine and serious adverse effects; all reports are related by time only. That is, they are only related because the effect happened some time after the vaccination. As of 1 September 2009, there have been 44 U.S. reports of death among females who have received the vaccine. None of the 27 confirmed deaths of women and girls who had taken the vaccine were linked to the vaccine. Guillain-Barré Syndrome (GBS), a rare disorder that causes muscle weakness, has been reported after vaccination with Gardasil. There is no evidence suggesting that Gardasil causes or raises the risk of GBS. Additionally, there have been rare reports of blood clots forming in the heart, lungs and legs.

As of 5 November 2009 the CDC continues to recommend Gardasil vaccination for the prevention of four types of HPV. Merck, the manufacturer of Gardasil, will continue to test women who have received the vaccine to determine the vaccine's efficacy over a lifetime.

History

In work that was initiated in the mid 1980s, the vaccine was developed, in parallel, by researchers at Georgetown University Medical Center, the University of Rochester, the University of Queensland in Australia, and the U.S. National Cancer Institute. In 2006, the U.S. Food and Drug Administration (FDA) approved the first preventive HPV vaccine, marketed by Merck & Co. under the trade name Gardasil. According to a Merck press release, in the second quarter of 2007, it had been approved in 80 countries, many under fast-track or expedited review. Early in 2007, GlaxoSmithKline filed for approval in the United States for a similar preventive HPV vaccine, known as Cervarix. In June 2007 this vaccine was licenced in Australia, and it was approved in the European Union in September 2007. Cervarix was approved for use in the U.S. in October 2009.

Prevalence of genital HPV

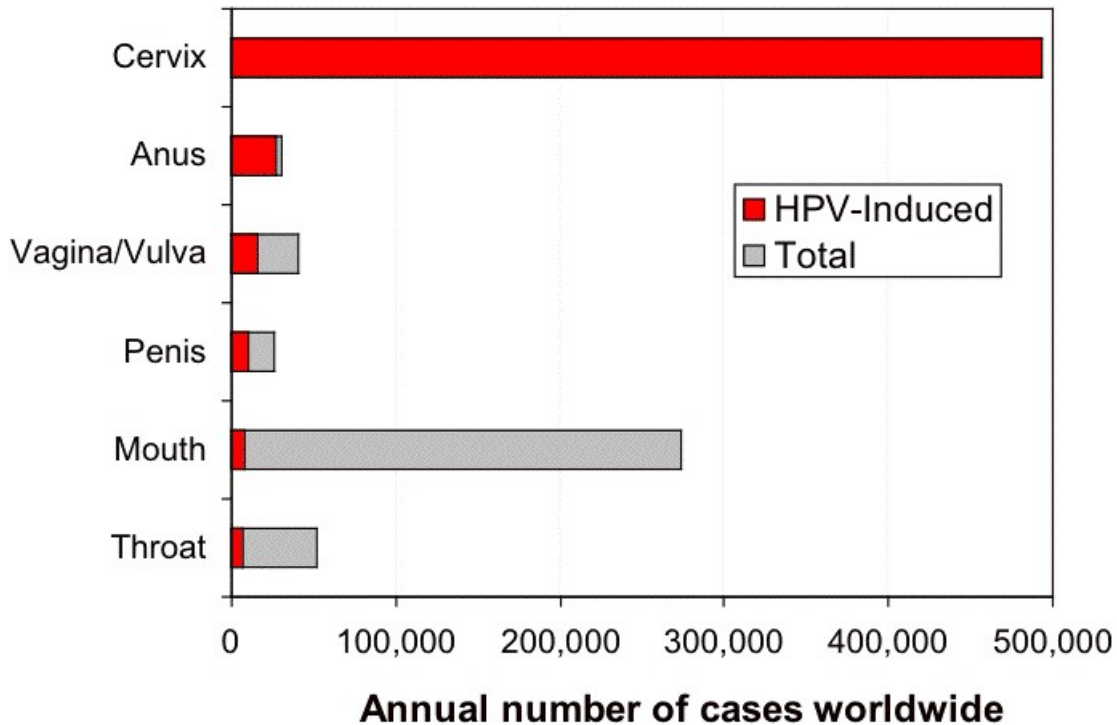
United States

According to the Centers for Disease Control and Prevention, by the age of 50 more than 80% of American women will have contracted at least one strain of genital HPV. Both men and women can be carriers of HPV. HPV is the most common sexually transmitted infection in the US. A large percentage of the American population is infected with genital HPV because HPV is highly communicable. As a result, American public health experts recommend widespread HPV vaccination.

At a given time, the overall prevalence of high-risk (cancer causing) HPV types was 15% of female participants; the prevalence of the types covered by the vaccine were 1.5% (HPV-16) and 0.8% (HPV-18). The overall prevalence of low-risk (wart causing) types was 18%, the two types covered by the vaccine were found in 1.3% (HPV-6) and 0.1% (HPV-11) of the population. Overall, the types prevented by the vaccine were found in 3.4% of female participants.

Only a small percentage of women with high-risk HPV develop cervical cancer. However, each year between 250,000 and 1 million American women are diagnosed with cervical dysplasia, which is caused by HPV and is a precursor to cervical cancer. Cervical dysplasia is painful and costly to treat.

About 11,000 American women are diagnosed with cervical cancer every year, and about 4,000 die per year of the disease. Most cancers occur in those who have not had Pap smears within the previous five years.



Estimated proportion of new cases of cancers attributable to HPV in 2002

There are 19 "high-risk" HPV types that can lead to the development of cervical cancer or other genital/anal cancers; some forms of HPV, particularly type 16, have been found to be associated with a form of throat cancer. Studies have found that human papillomavirus (HPV) infection is responsible for virtually all cases of cervical cancer.

Condoms protect against HPV, but do not completely prevent transmission. College freshmen women who used condoms consistently had a 37.8% per patient-year incidence of genital HPV, compared to an incidence of 89.3% among those who did not.

No data is kept by the U.S. government on genital wart incidence rates. It is estimated that in the U.S., at any one time about 1% of adults who have had sex have genital warts. It is estimated that about 20 million people are presently infected with HPV, and there are about six million new cases of HPV every year in the United States.

Worldwide

Worldwide, cervical cancer is the fifth most deadly cancer in women. There are an estimated 470,000 new cases of cervical cancer, and 233,000 deaths per year. Due to the success of Pap smear screening programs, the majority of cervical cancers and deaths occur in less developed parts of the world.

Vaccination and public health

Widespread vaccination has the potential to reduce cervical cancer deaths around the world by as much as two-thirds, if all women were to take the vaccine and if protection turns out to be long-term. In addition, the vaccines can reduce the need for medical care, biopsies, and invasive procedures associated with the follow-up from abnormal Pap tests, thus helping to reduce health care costs and anxieties related to abnormal Pap tests and follow-up procedures.

—American National Cancer Institute,

Comments made by Dr. Diane Harper, researcher for the HPV vaccines, were interpreted as indicating that in countries where Pap smear screening is common, it will take vaccination of a large proportion of women in order to further reduce cervical cancer rates.

Current preventive vaccines protect against the two HPV types (16 and 18) that cause about 70% of cervical cancers worldwide. Because of the distribution of HPV types associated with cervical cancer, the vaccines are likely to be most effective in Asia, Europe and North America. Some other high risk types cause a larger percentage of cancers in other parts of the world. Vaccines that protect against more of the types common in cancers would prevent more cancers, and be less subject to regional variation. For instance, a vaccine against the seven types most common in cervical cancers (16, 18, 45, 31, 33, 52, 58) would prevent an estimated 87% of cervical cancers worldwide.

Only 41% of women with cervical cancer in the developing world are able to access medical treatment for their illness. Therefore, prevention of HPV by vaccination may be a more effective way of lowering the disease burden in developing countries than cervical screening. The European Society of Gynecological Oncology sees the developing world as most likely to benefit from HPV vaccination. However, individuals in many resource-limited nations, Kenya for example, are unable to afford the vaccine.

Vaccine target populations

Gardasil and Cervarix are preventative vaccines and do not treat HPV infection or cervical cancer. They are recommended for women who are 9 to 25 years old who have not been exposed to HPV. However, since it is unlikely that a woman will have already contracted all four viruses, and because HPV is primarily sexually transmitted, the U.S. Centers for Disease Control and Prevention has recommended vaccination for women up to 26 years of age.

When Gardasil was first introduced, it was recommended as a prevention for cervical cancer for women that were 25 years old or younger. New evidence suggests that all Human Papillomavirus (HPV) vaccines are effective in preventing cervical cancer for women up to 45 years of age.

In November 2007, Merck presented new data on Gardasil. In an investigational study, Gardasil reduced incidence of HPV types 6, 11, 16 and 18-related persistent infection and disease in women through age 45. The study evaluated women who had not contracted at least one of the HPV types targeted by the vaccine by the end of the three-dose vaccination series. Merck planned to submit this data before the end of 2007 to the U.S. Food and Drug Administration (FDA), and to seek an indication for Gardasil for women through age 45.

Vaccination during pregnancy

In the Gardasil clinical trials, 1,115 pregnant women received the HPV vaccine. Overall, the proportions of pregnancies with an adverse outcome were comparable in subjects who received Gardasil and subjects who received placebo. However, the clinical trials had a relatively small sample size. Currently the vaccine is not recommended for pregnant women. The long-term effects of the vaccine on fertility are not known, but no effects are anticipated.

Vaccination of males

In the UK, HPV vaccines are licensed for boys aged 9–15. On 9 September 2009, an advisory panel recommended that the U.S. Food and Drug Administration (FDA) licence Gardasil in the United States for boys and men ages 9–26 for the prevention of genital warts. The vaccine has been FDA approved for use in males age 9 to 26 for prevention of genital warts, and anal cancer.

In males, Gardasil may reduce their risk of genital warts and precancerous lesions caused by HPV. This reduction in precancerous lesions might be predicted to reduce the rates of penile and anal cancer in men. Since penile and anal cancers are much less common than cervical cancer, HPV vaccination of young men is likely to be much less cost-effective than for young women. From a public health point of view, vaccinating men as well as women decreases the virus pool within the population, but is only cost-effective if the uptake in the female population is extremely low. In the United States, the cost per quality-adjusted life year is greater than \$100,000 for vaccinating the male population, compared to the less than \$50,000 for vaccinating the female population. This assumes a 75% vaccination rate.

Gardasil is in particular demand among gay men, who are at higher risk for genital warts, penile cancer, and anal cancer.

As with females, the vaccine should be administered before infection with the HPV types covered by the vaccine occurs. Vaccination before adolescence therefore makes it more likely that the recipient has not been exposed to HPV.

Mechanism of action

The latest generation of preventive HPV vaccines is based on hollow virus-like particles (VLPs) assembled from recombinant HPV coat proteins. The vaccines target the two high-risk HPVs, types 16 and 18 that cause the most cervical cancers. Together, these two HPV types currently cause about 70 percent of all cervical cancer. Gardasil also targets HPV types 6 and 11, which together currently cause about 90 percent of all cases of genital warts.

Gardasil and Cervarix are designed to elicit virus-neutralizing antibody responses that prevent initial infection with the HPV types represented in the vaccine. The vaccines have been shown to offer 100 percent protection against the development of cervical pre-cancers and genital warts caused by the HPV types in the vaccine, with few or no side effects. The protective effects of the vaccine are expected to last a minimum of 4.5 years after the initial vaccination.

While the study period was not long enough for cervical cancer to develop, the prevention of these cervical precancerous lesions (or dysplasias) is believed highly likely to result in the prevention of those cancers.

Research directions

There are high-risk HPV types are not affected by the vaccines. Ongoing research is focused on the development of HPV vaccines that will offer protection against a broader range of HPV types.

There is also substantial research interest in the development of therapeutic vaccines, which seek to elicit immune responses against established HPV infections and HPV-induced cancers.

Therapeutic HPV vaccines

In addition to preventive vaccines, such as Gardasil and Cervarix, laboratory research and several human clinical trials are focused on the development of therapeutic HPV vaccines. In general these vaccines focus on the main HPV oncogenes, E6 and E7. Since expression of E6 and E7 is required for promoting the growth of cervical cancer cells (and cells within warts), it is hoped that immune responses against the two oncogenes might eradicate established tumors.

Vaccine implementation

In developed countries, the widespread use of cervical "Pap smear" screening programs has reduced the incidence of invasive cervical cancer by 50% or more. Current preventive vaccines reduce, but do not eliminate the chance of getting cervical cancer. Therefore,

experts recommend that women combine the benefits of both programs by seeking regular Pap smear screening, even after vaccination.

Australia

Commencing in 2007 The Australian federal government began funding a voluntary program to make the Gardasil vaccine available free of charge to women aged 12–26 for a period of two years, with an ongoing vaccination program for 12- and 13-year-olds as part of the pre-existing high school vaccination program.

The Australian government and the PBS (Pharmaceutical Benefits Scheme) have approved the vaccine for use and in 2007 began a nationwide vaccination program free of charge to schoolgirls in years 7 to 12. These programs are run by local councils with funding and vaccine supplies from the government. The subsidization approval process, however, appears to have been heavily influenced by political interference from politicians of all political parties, and by the Prime Minister who publicly advised that it would be approved (before approval). In addition, women between 18 and 26 years of age at the time of the first dose may receive the vaccine for free upon request from their general practitioner. After June 2009, the program will be scaled down to 12- and 13-year-old girls only. Australia also approved Gardasil for boys 9–15 years old, but Australia is not providing government funding for vaccinating boys.

Canada

Canada has approved use of Gardasil. Initiating and funding free vaccination programs has been left to individual Province/Territory Governments. In the provinces of Ontario, Prince Edward Island, Newfoundland and Nova Scotia, free vaccinations to protect women against HPV were slated to begin in September 2007 and will be offered to girls ages 11–14. Similar vaccination programs are being planned in British Columbia and Quebec.

France

On July 17, 2007, France issued a directive authorizing state-aided voluntary vaccination for girls aged 14–23 years who have not yet become sexually active, or have been sexually active for less than a year. The state refunds 65% of the cost, based on a program of 3 vaccinations at €135 (slightly less than \$200) per shot, meaning that the patient covers €141.75 (slightly more than \$200).

Germany and Italy

On March 26, 2007, early approval for Gardasil vaccinations was granted in both Germany and Italy.

Greece

On February 12, 2007, Greece made HPV vaccination mandatory for girls entering gymnasium (7th grade). All vaccines including hepatitis B are mandatory and are supplied free to everyone in Greece, with parents being allowed to opt out of vaccinating their kids. Cervarix and Gardasil are supplied free to all girls and women between the ages of 12 and 26.

Kenya

Both Cervarix and Gardasil are approved for use within Kenya by the Pharmacy and Poisons Board. However, at a cost of 20,000 Kenyan shillings, which is more than the average annual income for a family, the director of health promotion in the Ministry of Health, Nicholas Muraguri, states that many Kenyans are unable to afford the vaccine.

New Zealand

The publicly-funded New Zealand HPV Immunisation Programme began on 1 September 2008. Gardasil is available free for New Zealand girls and young women born on or after 1 January 1990 through general practices, some family planning clinics and participating schools. HPV immunization is part of the regular immunization schedule for girls in year 8 at school (or age 12 if not delivered through a school-based programme). There is also a catch-up programme for older girls. Girls born in 1990 and 1991 have until 31 December 2011 to start the programme for free. Girls born from 1992 onwards have until their 20th birthday to start the programme for free. Over 82,000 New Zealand girls and young women have chosen to get the HPV immunisation in the programme's first year.

Norway

In Norway, starting from the fall of 2009, HPV vaccination was introduced into the national immunisation programme, for girls aged 12–13. In March 2010, 57% of all girls born in 1997 had received the first dose of the vaccine.

Romania

In November 2008, Romanian authorities launched a campaign to vaccinate 110,000 girls aged 10 and 11. The Ministry of Health acquired 330,000 vaccine doses for 23 million euros. By an order of the Ministry, the girls' parents must approve or reject the vaccination in writing, and must "fully assume the consequences for their children" if they reject the vaccination.

South Korea

On July 27, 2007, South Korean government approved Gardasil for use in girls and women aged 9 to 26 and boys aged 9 to 15. Approval for use in boys was based on safety and immunogenicity but not efficacy.

Sweden

In Sweden, starting January 1, 2010, girls born in the year 1999 or later and in the ages 10 to 12 can receive a free HPV vaccine.

United Kingdom

In the UK the vaccine is licensed for girls aged 9 to 15 and for women aged 16 to 26.

HPV vaccination with Cervarix was introduced into the national immunisation programme in September 2008, for girls aged 12–13 across the UK. A two-year catch up campaign started in Autumn 2009 to vaccinate all girls up to 18 years of age. Catch up vaccination will be offered to:

- girls aged between 16 and 18 from autumn 2009, and
- girls aged between 15 and 17 from autumn 2010.

By the end of the catch up campaign, all girls under 18 will have been offered the HPV vaccine. Women over the age of 18 are not included in the programme as it would not be cost effective in preventing cervical cancer.

It will be many years before the vaccination programme has an effect upon cervical cancer incidence so women are advised to continue accepting their invitations for cervical screening.

United States

The cost of HPV vaccine for females under 18 who are uninsured is covered under the federal Vaccines for Children Program.

As of late 2007, about one quarter of US females age 13–17 years had received at least one of the three HPV shots.

According to the US Centers for Disease Control and Prevention (CDC), getting as many girls vaccinated as early and as quickly as possible will reduce the cases of cervical cancer among middle-aged women in 30 to 40 years and reduce the transmission of this highly communicable infection. Barriers include the limited understanding by many people that HPV causes cervical cancer, the difficulty of getting pre-teens and teens into the doctor's office to get a shot, and the high cost of the vaccine (\$120/dose, \$360 total for the three required doses, plus the cost of doctor visits).

Legislation

Shortly after the first HPV vaccine was approved, bills to include the vaccine among those that are mandatory for school attendance were introduced in many states. Only two such bills passed (in Virginia and Washington DC) during the first four years after

vaccine introduction. Mandates have been effective at increasing uptake of other vaccines, such as mumps, measles, rubella, and hepatitis B (which is also sexually transmitted).ref name=pmid_17380109 /> However most such efforts developed for five or more years after vaccine release, while financing and supply were arranged, further safety data was gathered, and education efforts increased understanding, before mandates were considered.

Other measures that have been considered include requiring insurers to cover HPV vaccination, and funding HPV vaccines for those without insurance. The opt-out policy in Virginia is so broad that the legislation there hardly counts as a mandate.

Opt-out policies

Almost all pieces of legislation currently pending in the states that would make the vaccine mandatory for school entrance have an "opt-out" policy.

State-by-State

The National Conference of State Legislatures periodically issues summaries of HPV vaccine related legislation.

Other states are also preparing bills to handle issuing the HPV Vaccine.

State	Proposal	Status	Opt Out Policy
Alaska	Voluntary vaccination program	Passed	Not Applicable
District of Columbia	Bill would require girls to be vaccinated before they turn 13 to attend school.	Passed	Yes
Nevada	Bill would require health insurance companies to cover the cost of the vaccine	Passed into law	Not Applicable
New Hampshire	Voluntary program provides vaccine free of charge to girls between the ages of eleven and eighteen.	Passed and presently in effect.	Yes
Texas	Governor issued executive order requiring that girls entering the sixth grade be vaccinated.	Texas legislature overrode executive order and barred mandatory vaccination until at least 2011.	Yes
Virginia	Bill requires girls entering the sixth grade to be	Passed the legislature. Goes into effect Oct. 1,	Yes

vaccinated.

2008; to be implemented in fall of 2009.

Immigrants

Between July 2008 and December 2009, proof of the first of three doses of HPV Gardasil vaccine was required for women ages 11-26 intending to legally enter the United States. This requirement stirred controversy because of the cost of the vaccine, and because all the other vaccines so required prevent diseases which are spread by respiratory route and considered highly contagious. The Centers for Disease Control and Prevention repealed all HPV vaccination directives for immigrants effective December 14th, 2009.

Opposition in the United States

Health insurance companies

There has been significant opposition from health insurance companies to covering the cost of the vaccine (\$360).

Religious right and conservative groups

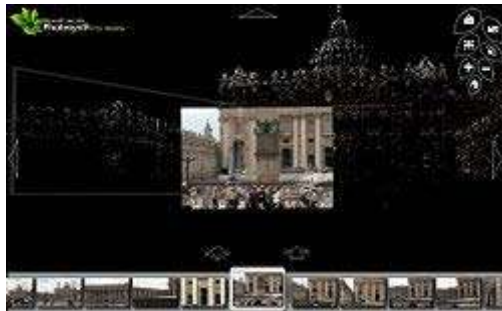
Several conservative groups in the U.S. have publicly opposed the concept of making HPV vaccination mandatory for pre-adolescent girls, asserting that making the vaccine mandatory is a violation of parental rights. They also say that it will lead to early sexual activity, giving a false sense of immunity to sexually transmitted disease. Both the Family Research Council and the group Focus on the Family support widespread (universal) availability of HPV vaccines but oppose mandatory HPV vaccinations for entry to public school.

Many organizations disagree with the argument that the vaccine increases sexual activity among teens. Dr. Christine Peterson, director of the University of Virginia's Gynecology Clinic, said "The presence of seat belts in cars doesn't cause people to drive less safely. The presence of a vaccine in a person's body doesn't cause them to engage in risk-taking behavior they would not otherwise engage in."

Chapter- 6

Photosynth

Microsoft Photosynth



Photosynth technology preview showing Piazza San Pietro,
Vatican City

Developer(s)	Microsoft
Stable release	2.110.317.1042 / March 18, 2010; 10 months ago
Type	3D modelling, Panorama stitching

Photosynth is a software application from Microsoft Live Labs and the University of Washington that analyzes digital photographs and generates a three-dimensional model of the photos and a point cloud of a photographed object. Pattern recognition components compare portions of images to create points, which are then compared to convert the image into a model. Users are able to view and generate their own models using a software tool available for download at the Photosynth website.

History

Photosynth is based on Photo Tourism, a research project by University of Washington graduate student Noah Snavely. Shortly after Microsoft's acquisition of Seadragon in early 2006, that team began work on Photosynth, under the direction of Seadragon founder Blaise Agueria y Arcas.

Microsoft released a free tech preview version on November 9, 2006. Users could view models generated by Microsoft or the BBC, but not create their own models at that time. Microsoft teamed up with NASA on August 6, 2007 allowing users to preview its Photosynth technology showing the Space Shuttle Endeavour. On August 20, 2007, a preview showing the tiles of Endeavour during the backflip process was made available for viewing.

On August 20, 2008, Microsoft officially released Photosynth to the public, allowing users to upload their images and generate their own Photosynth models.

In March 2010, Photosynth added support for Gigapixel panoramas stitched in Microsoft ICE. The panoramas use Seadragon based technology similar to the system already used in synths.

Process

The Photosynth technology works in two steps. The first step involves the analysis of multiple photographs taken of the same area. Each photograph is processed using an interest point detection and matching algorithm developed by Microsoft Research which is similar in function to UBC's Scale-invariant feature transform. This process identifies specific features, for example the corner of a window frame or a door handle. Features in one photograph are then compared to and matched with the same features in the other photographs. Thus photographs of the same areas are identified. By analyzing the position of matching features within each photograph, the program can identify which photographs belong on which side of others. By analyzing subtle differences in the relationships between the features (angle, distance, etc.), the program identifies the 3D position of each feature, as well as the position and angle at which each photograph was taken. This process is known scientifically as Bundle adjustment and is commonly used in the field of photogrammetry, with similar products available such as Imodeller and D-Sculptor. This first step is extremely computationally intensive, but only has to be performed once on each set of photographs.

The second step involves the display of and navigation through the 3D point cloud of features identified in the first step. This is done with the publicly downloadable Photosynth viewer. The viewer resides on a client computer and maintains a connection to a server that stores the original photographs. It enables a user to, among other things, see any of the photographs from their original vantage point. It incorporates DeepZoom technology Microsoft obtained through its acquisition of Seadragon in January 2006. The

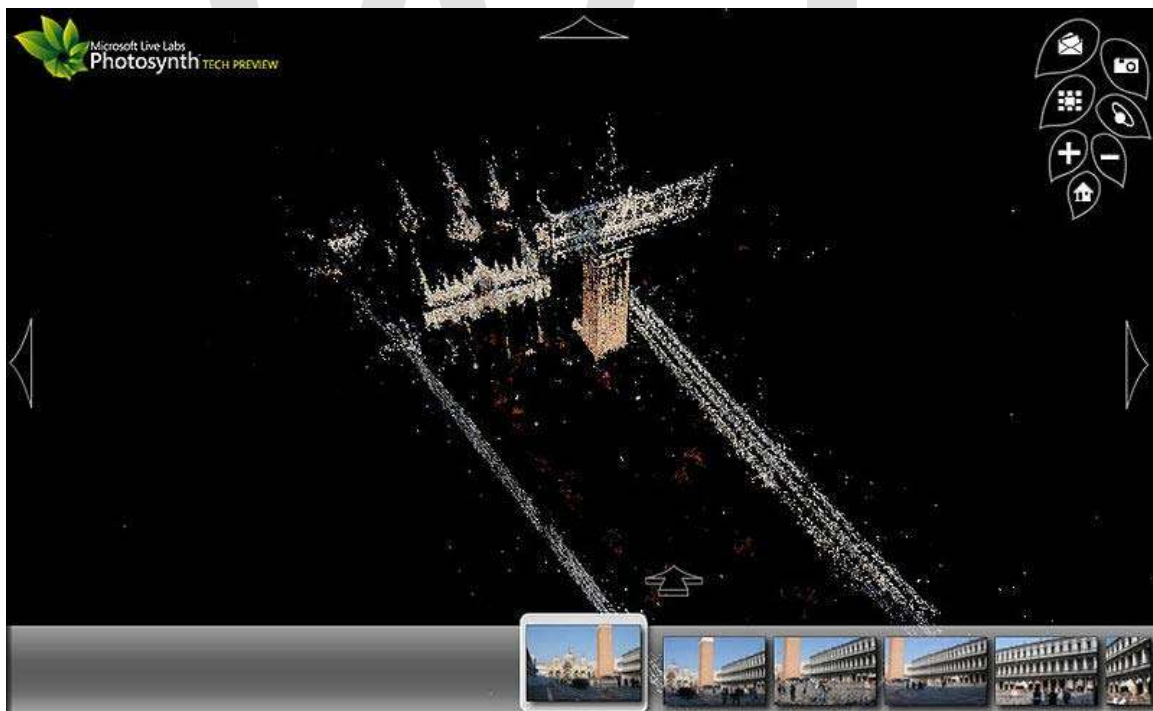
Seadragon technology enables smooth zooming into the high-resolution photographs without downloading them to the user's machine.

The Photosynth Direct 3D-based viewing software is only available to the Windows 7, Windows Vista and Windows XP operating systems. However, the team released a Silverlight version of the viewer which has succeeded the D3D viewer as the main option to view photosynths.

As of March 2009 user uploaded Photosynth collections are now available for viewing on iPhones using iSynth (3D) or Seadragon Mobile (2D only).

Capabilities

Current generation photosynths are easy to capture, as photographs uploaded on Photosynth can be taken by any regular digital camera or mobile phone. In general, the higher the megapixels, the clearer the pictures. Users have the option to geotag their digital shots on sites such as Flickr and then upload them on the online Photosynth web service. Images uploaded on Photosynth give people the ability to seamlessly view landmarks, public spaces and objects from all sides.



model view of Piazza San Marco, Venice

Chapter- 7

Boeing 787

Boeing 787 Dreamliner



The first Boeing 787-8 *Dreamliner* on its maiden flight

Role	Wide-body jet airliner
National origin	United States, with international partners
Manufacturer	Boeing Commercial Airplanes
First flight	December 15, 2009
Status	In development, flight testing and early production
Number built	7
Unit cost	787-8: US\$185.2 million (2010) 787-9: US\$218.1 million (2010)

The **Boeing 787 Dreamliner** is a long-range, mid-size, wide-body, twin-engine jet airliner developed by Boeing Commercial Airplanes. It seats 210 to 330 passengers, depending on the variant. Boeing states that it is the company's most fuel-efficient airliner and the world's first major airliner to use composite materials for most of its construction. The 787 consumes 20% less fuel than the similarly-sized Boeing 767. Some of its distinguishing features include a four-panel windshield, noise-reducing chevrons on its engine nacelles, and a smoother nose contour.

The aircraft's initial designation 7E7 was changed to 787 in January 2005. The first 787 was unveiled in a roll-out ceremony on July 8, 2007, at Boeing's Everett assembly factory, by which time it had become the fastest-selling wide-body airliner in history with 677 orders. By September 2010, 847 Boeing 787s had been ordered by 56 customers. As of 2010, launch customer All Nippon Airways has the largest number of 787s on order.

The 787 development and production has involved a large-scale collaboration with numerous suppliers around the globe. It is being assembled at the Boeing Everett Factory in Everett, Washington. Aircraft will also be assembled at a new factory in North Charleston, South Carolina. Both sites will deliver 787s to airline customers. Originally planned to enter service in May 2008, the project has suffered from repeated delays and is now more than three years behind schedule. The airliner's maiden flight took place on December 15, 2009, and it is currently undergoing flight testing with a goal of receiving certification in mid-2011 and entering service in 2011.

Development

Background

During the late 1990s, Boeing began considering replacement aircraft programs as sales for the 767 and Boeing 747-400 slowed. The company proposed two new aircraft, the 747X, which would have lengthened the 747-400 and improved efficiency, and the Sonic Cruiser, which would have achieved 15% higher speeds (approximately Mach 0.98) while burning fuel at the same rate as the existing 767. Market interest for the 747X was tepid, but the Sonic Cruiser had brighter prospects. Several major airlines in the United States, including Continental Airlines, initially showed enthusiasm for the Sonic Cruiser concept, although they also expressed concerns about the operating cost.



Earlier proposed design configuration of the Boeing 7E7

The global airline market was upended by the September 11, 2001 attacks and increased petroleum prices, making airlines more interested in efficiency than speed. The worst-affected airlines, those in the United States, had been considered the most likely

customers of the Sonic Cruiser, and thus Boeing officially canceled the Sonic Cruiser on December 20, 2002. Switching tracks, the company announced an alternative product using Sonic Cruiser technology in a more conventional configuration, the 7E7, on January 29, 2003. The emphasis on a smaller midsize twinjet rather than a large 747-size aircraft represented a shift from hub-and-spoke theory towards the point-to-point theory, in response to analysis of focus groups.

“ The 7E7 looks fairly traditional on the outside, but it will be dramatically different on the inside. ”

—*Time*

The replacement for the Sonic Cruiser project was dubbed the "7E7" (with a development code name of "Y2"). Technology from the Sonic Cruiser and 7E7 was to be used as part of Boeing's project to replace its entire airliner product line, an endeavor called the Yellowstone Project (of which the 7E7 became the first stage). Early concept images of the 7E7 included rakish cockpit windows, a dropped nose and a distinctive "shark-fin" tail. The "E" was said to stand for various things, such as "efficiency" or "environmentally friendly"; however, in the end, Boeing claimed that it stood merely for "Eight". In July 2003, a public naming competition was held for the 7E7, for which out of 500,000 votes cast online the winning title was *Dreamliner*. Other names in the pool included *eLiner*, *Global Cruiser* and *Stratoclimber*.

Design effort

On April 26, 2004, Japanese airline All Nippon Airways became the launch customer for the 7E7 Dreamliner, by announcing a firm order for 50 aircraft with deliveries to begin in late 2008. All Nippon Airways's order was initially specified as 30 787-3, 290–330 seat, one-class domestic aircraft, and 20 787-8, long-haul, 210–250 seat, two-class aircraft for regional international routes such as Tokyo Narita–Beijing. The aircraft would allow All Nippon Airways to open new routes to cities not previously served, such as Denver, Moscow, and New Delhi. The 787-3 and 787-8 were to be the initial variants, with the 787-9 entering service in 2010.



All Nippon Airways launched the 787 Dreamliner program with an order for 50 aircraft in 2004. This aircraft made an emergency landing during a test flight in Texas, on November 9, 2010.

The 787 was designed to become the first production composite airliner, with the fuselage assembled in one-piece composite barrel sections instead of the multiple aluminum sheets and some 50,000 fasteners used on existing aircraft. Boeing selected two new engine types to power the 787, the General Electric GENx and Rolls-Royce Trent 1000. Boeing claimed the 787 would be near to 20% more fuel-efficient than the 767, with one-third of the efficiency gain from the engines, another third from aerodynamic improvements and the increased use of lighter-weight composite materials, and the final third from advanced systems.

During the design phase, the 787 underwent extensive wind tunnel testing at Boeing's Transonic Wind Tunnel, QinetiQ's five-meter wind tunnel at Farnborough, UK, and NASA Ames Research Center's wind tunnel, as well as at the French aerodynamics research agency, ONERA. The final styling of the aircraft was more conservative than earlier proposals, with the fin, nose, and cockpit windows changed to a more conventional form. By the end of 2004, customer-announced orders and commitments for the 787 reached 237 aircraft. Boeing initially priced the 787-8 variant at US\$120 million, a low figure that surprised the industry. In 2007, the list price was US\$146–151.5 million for the 787-3, US\$157–167 million for the 787-8 and US\$189–200 million for the 787-9.

Manufacturing and suppliers

After stiff competition, Boeing announced on December 16, 2003, that the 787 would be assembled in its factory in Everett, Washington. Instead of building the complete aircraft from the ground up in the traditional manner, final assembly would employ just 800 to 1,200 people to join completed subassemblies and to integrate systems. Boeing assigned its global subcontractors to do more assembly themselves and deliver completed subassemblies to Boeing for final assembly. This approach was intended to result in a leaner and simpler assembly line and lower inventory, with pre-installed systems reducing final assembly time by three-quarters to three days.



Assembly of Section 41 of a Boeing 787

Subcontracted assemblies included wing manufacture (Mitsubishi Heavy Industries, Japan, central wing box) horizontal stabilizers (Alenia Aeronautica, Italy; Korea Aerospace Industries, South Korea); fuselage sections (Global Aeronautica, Italy; Boeing, North Charleston, USA; Kawasaki Heavy Industries, Japan; Spirit AeroSystems, Wichita, USA; Korean Air, South Korea); passenger doors (Latécoère, France); cargo doors, access doors, and crew escape door (Saab, Sweden); floor beams (TAL Manufacturing Solutions Limited, India); wiring (Labinal, France); wing-tips, flap support fairings, wheel well bulkhead, and longerons (Korean Air, South Korea); landing gear (Messier-Dowty, France); and power distribution and management systems, air conditioning packs (Hamilton Sundstrand, Connecticut, USA). Boeing is considering

bringing construction of the 787-9 tail "in house"; the tail of the 787-8 is currently made by Alenia.

To speed delivery of the 787's major components, Boeing modified several used 747-400s into 747 Dreamlifters to transport 787 wings, fuselage sections, and other smaller parts. Japanese industrial participation was very important to the project, with a 35% work share, the first time Japanese firms had taken a lead role in mass production of Boeing airliner wings, and many of the subcontractors supported and funded by the Japanese government. On 26 April 2006, Japanese manufacturer Toray Industries and Boeing announced a production agreement involving US\$6 billion worth of carbon fiber, extending a 2004 contract and aimed at easing production concerns.

Production and delivery delays

Boeing had originally planned for a first flight by the end of August 2007 and premiered the first 787 at a rollout ceremony on July 8, 2007, which matches the aircraft's designation in the US-style month-day-year format (7/8/07). However, the aircraft's major systems had not been installed at that time, and many parts were attached with temporary non-aerospace fasteners requiring their later replacement with flight fasteners. Although intended to shorten the production process, 787 subcontractors initially had difficulty completing the extra work, because they could not procure the needed parts, perform the subassembly on schedule, or both, leaving remaining assembly work for Boeing to complete as "traveled work".



The 787 Dreamliner's first public appearance was webcast live on July 8, 2007.

On September 5, Boeing announced a three-month delay, blaming a shortage of fasteners as well as incomplete software. On October 10, 2007, a second three-month delay to the first flight and a six-month delay to first deliveries was announced due to problems with the foreign and domestic supply chain, including an ongoing fastener shortage, the lack of documentation from overseas suppliers, and continuing delays with the flight guidance software. Less than a week later, Mike Bair, the 787 program manager was replaced. On January 16, 2008, Boeing announced a third three-month delay to the first flight of the 787, citing insufficient progress on "traveled work". On March 28, 2008, in an effort to gain more control over the supply chain, Boeing announced that it planned to buy Vought Aircraft Industries' interest in Global Aeronautica; the company later agreed to also purchase Vought's North Charleston, S.C. factory.

On April 9, 2008, Boeing officially announced a fourth delay, shifting the maiden flight to the fourth quarter of 2008, and delaying initial deliveries by around 15 months to the third quarter of 2009. The 787-9 variant was postponed to 2012 and the 787-3 variant was to follow with no firm delivery date. On November 4, 2008, the company announced a fifth delay due to incorrect fastener installation and the Boeing machinists strike, stating that the first test flight would not occur in the fourth quarter of 2008. After assessing the 787 program schedule with its suppliers, Boeing confirmed on December 11, 2008 that the first flight would be delayed until the second quarter of 2009.

On June 15, 2009, during the Paris Air Show, Boeing said that the 787 would make its first flight within two weeks. However, on June 23, 2009, Boeing announced that the first flight is postponed "due to a need to reinforce an area within the side-of-body section of the aircraft". Boeing provided an updated 787 schedule on August 27, 2009, with the first flight planned to occur by the end of 2009 and deliveries to begin at the end of 2010. The company expects to write off US\$2.5 billion because it considers the first three Dreamliners built unsellable and suitable only for flight tests.

Boeing announced on July 15, 2010, that the first delivery to launch customer All Nippon Airways could slip into 2011, and on August 27, 2010 it confirmed that the first delivery would be delayed until early 2011. Boeing and Rolls-Royce state a lack of Trent 1000 engines as the cause, following shutdown of Rolls-Royce's test facility after a blowout in a Trent 1000 during ground testing on August 2. In August 2010, it was announced that Boeing was facing a US\$1 billion compensation claim from Air India due to the delays for the 27 Dreamliners it has on order.

In early November 2010, it was reported that some early 787 deliveries may be delayed, in one case some three months, to allow for rework to address issues found during flight testing. In January 2011, Boeing announced that the first 787 delivery was rescheduled to the third quarter of 2011 due to software and electrical updates following the in-flight fire in November 2010.

Pre-flight ground testing



The first Boeing 787 underwent taxi tests at Paine Field in November and December 2009.

As Boeing worked with its suppliers on early 787 production, the aircraft design had proceeded through a series of test goals. On August 7, 2007, on-time certification of the Rolls-Royce Trent 1000 engine by European and US regulators was received. On August 23, 2007, a crash test involving a vertical drop of a partial composite fuselage section from about 15 ft (4.6 m) onto a 1 in (25 mm)-thick steel plate occurred in Mesa, Arizona; the results matched what Boeing's engineers had predicted, allowing modeling of various crash scenarios using computational analysis instead of further physical tests.

The alternative GE GENx-1B engine achieved certification on March 31, 2008. On June 20, 2008, the 787 team achieved "Power On" of the first aircraft, powering and testing the aircraft's electrical supply and distribution systems. A non-flight 787 test airframe was built for static testing, and on September 27, 2008, over a period of nearly two hours, the fuselage was successfully tested at 14.9 psi (102.7 kPa), which is 150 percent of the maximum pressure expected in commercial service (i.e., when flying at maximum cruising altitude). In December 2008, the Federal Aviation Administration (FAA) passed the maintenance program for the 787.

On May 3, 2009, the first test 787 was moved to the flight line following extensive factory-testing, including landing gear swings, systems integration verification, and a total run-through of the first flight. Boeing spent most of May 2009 conducting tests on the first 787 in preparation for the first flight. On March 28, 2010, the 787 completed the

ultimate wing load test, which requires that the wings of a fully assembled aircraft be loaded to 150% of design limit load and held for 3 seconds. The wings were flexed approximately 25 ft (7.6 m) upward during the test. Unlike past aircraft however, the wings were not tested to failure. On April 7, Boeing announced that analysis of the data showed the test was a success. On December 12, 2009, the first 787 completed high speed taxi tests, the last major step before flight.



Takeoff of the first Boeing 787 built on its maiden flight

Flight test program

On December 15, 2009, Boeing conducted the Dreamliner's maiden flight with the first 787-8, originating from Snohomish County Airport in Everett, Washington at 10:27 am PST, and landing at Boeing Field in King County, Washington at 1:35 pm PST. Originally scheduled for four hours, the test flight was shortened to three hours because of bad weather. Boeing's schedule called for a 9-month flight test campaign (later revised to 8.5 months). The company's previous major aircraft, the 777, took 11 months with nine aircraft, partly to demonstrate 180-min ETOPS, one of its main features.

The 787 flight test program is composed of 6 aircraft, ZA001 through ZA006, four with Rolls-Royce Trent 1000 engines and two with GE GENx-1B64 engines. The second 787, ZA002 in All Nippon Airways livery, flew to Boeing Field on December 22, 2009 to join the flight test program; the third 787, ZA004 joined the test fleet with its first flight on February 24, 2010, followed by ZA003 on March 14, 2010. On March 24, 2010, testing for flutter and ground effects was completed, clearing the aircraft to fly its entire flight envelope.



The first 787 to visit Europe, ZA003 on display at the 2010 Farnborough Airshow

On April 23, 2010 Boeing delivered their latest 787 to a hangar at Eglin Air Force Base, Florida for extreme weather testing in temperatures ranging from 115 °F to -45 °F (46 °C to -42 °C), with all steps necessary to prepare for takeoff taken once the plane stabilizes at either temperature extreme. Dreamliner ZA005, the fifth 787 and the first with General Electric GENx engines began ground engine tests in May 2010. ZA005 made its first flight on June 16, 2010 and joined the flight test program. In June 2010, gaps were discovered in the horizontal stabilizers of test aircraft, due to improperly installed shims; all aircraft produced then were to be inspected and repaired. The 787 made its first appearance at an international air show at the Farnborough Airshow, UK on July 18, 2010.

In September 2010, it was reported that a further two 787s might join the test fleet, making a total of eight flight test aircraft. On September 10, 2010, a partial engine surge or runaway occurred in a Trent engine on ZA001 at Roswell. On October 4, 2010, the sixth 787, ZA006 joined the test program with its first flight. As of November 8, 2010, the six 787 test aircraft have flown 2,290 hours in 735 flights combined.

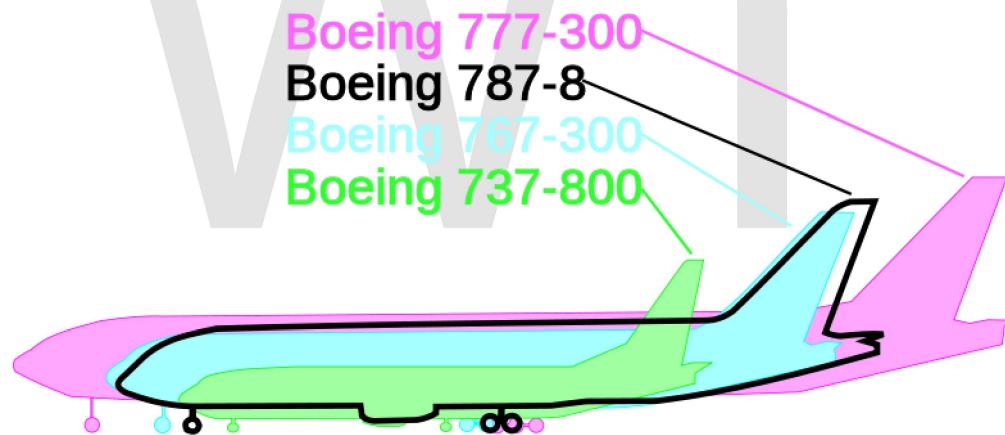
On November 9, 2010, Boeing 787, ZA002 made an emergency landing after smoke and flames were detected in the main cabin during a test flight over Texas. A Boeing spokeswoman said the airliner landed safely and the crew was evacuated after landing at the Laredo International Airport, Texas. The electrical fire caused some systems to fail before landing. Following this incident, Boeing suspended flight testing on November 10, 2010. Ground testing has been performed instead. On November 22, 2010, Boeing announced that the in-flight fire can be primarily attributed to foreign object debris (FOD) that was present in the electrical bay. After electrical system and software

changes, the 787 resumed company flight testing on December 23, 2010. Certifications by the European Aviation Safety Agency are expected by the end of 2011.

Design

The longest-range 787 variant can fly 8,000 to 8,500 nautical miles (14,800 to 15,700 km), enough to cover the Los Angeles to Bangkok or New York City to Taipei routes. It will have a cruising airspeed of Mach 0.85 (561 mph, 903 km/h at typical cruise altitudes). External features include raked wingtips and engine nacelles with noise-reducing serrated edges. The two different engine models compatible with the 787 use a standard electrical interface to allow an aircraft to be fitted with either Rolls-Royce or General Electric engines. This aims to save time and cost when changing engine types; while previous aircraft can have engines changed to those of a different manufacturer, the high cost and time required makes it rare. In 2006, Boeing addressed reports of an extended change period by stating that the 787 engine swap was intended to take 24 hours; engine interchangeability, it is reported, makes the 787 a more flexible asset to airlines, allowing them to change easily from one manufacturer's engine to the other if required.

Airframe



Size comparison of the Boeing 787-8 (**black outline**) with the Boeing 777-300 (**pink**), 767-300 (**cyan**), and 737-800 (**green**).

The 787 features lighter-weight construction. Its materials (by weight) are: 50% composite, 20% aluminum, 15% titanium, 10% steel, 5% other.; the craft will be 80% composite by volume. Each 787 contains approximately 35 short tons of carbon fiber reinforced plastic (CFRP), made with 23 tons of carbon fiber. Aluminum is used on wing and tail leading edges, titanium used mainly on engines and fasteners, with steel used in various places.

Carbon fiber composites have a higher strength-to-weight ratio than traditional aircraft materials, and help make the 787 a lighter aircraft. Composites are used on fuselage,

wings, tail, doors, and interior. Boeing had built and tested the first commercial aircraft composite section while examining the Sonic Cruiser concept nearly five years before; the Bell Boeing V-22 Osprey military transport uses over 50% composites, and the C-17 has over 16,000 lb (7,300 kg) of structural composites.

In 2006, Boeing launched the 787 GoldCare program. This is an optional, comprehensive life-cycle management service whereby aircraft in the program are routinely monitored and repaired as needed. This is the first program of its kind from Boeing: Post-sale protection programs are not new, but have usually been offered by third party service centers. Boeing is also designing and testing composite hardware so inspections are mainly visual. This will reduce the need for ultrasonic and other non-visual inspection methods, saving time and money.



Boeing 787 flight deck

Flight systems

On the 787, Honeywell and Rockwell-Collins provide flight control, guidance, and other avionics systems, including standard dual head up guidance systems, while Thales supplies the integrated standby flight display and electrical power conversion system. A version of Ethernet (Avionics Full-Duplex Switched Ethernet (AFDX) / ARINC 664) will be used to transmit data between the flight deck and aircraft systems. The flight deck

features LCD multi-function displays, all of which will use an industry standard GUI widget toolkit (Cockpit Display System Interfaces to User Systems / ARINC 661). The Lockheed Martin Orion spacecraft will use a glass cockpit derived from Honeywell International's 787 flight deck. The 787 flight deck includes two head-up displays (HUDs) as a standard feature. Like other Boeing airliners, the 787 will use a yoke instead of a side-stick. The future integration of forward looking infrared into the HUD system for thermal sensing so the pilots can "see" through the clouds is under consideration.



Angled planform view of the second 787 Dreamliner during flight testing

The most notable contribution to efficiency is the new electrical architecture, which replaces bleed air and hydraulic power sources with electrically powered compressors and pumps, as well as completely eliminating pneumatics and hydraulics from some subsystems (e.g., engine starters or brakes). The 787's engines use all-electrical bleedless systems, eliminating the superheated air conduits normally used for aircraft power, de-icing, and other functions. Another new system is a wing ice protection system that uses electro-thermal heater mats on the wing slats instead of hot bleed air that has been traditionally used.

An active gust alleviation system, similar to the system used on the B-2 bomber, improves ride quality during turbulence. Boeing, as part of its "Quiet Technology Demonstrator 2" project, is experimenting with several engine noise-reducing technologies for the 787. Among these are a redesigned air inlet containing sound-absorbing materials and redesigned exhaust duct covers whose rims are tipped in a

toothed pattern to allow for quieter mixing of exhaust and outside air. Boeing expects these developments to make the 787 significantly quieter both inside and out.

Interior

The 787-8 is designed to seat 234 passengers in a three-class setup, 240 in two-class domestic configuration, and 296 passengers in a high-density economy arrangement. Seat rows can be arranged in four to six abreast in first or business (e.g. 1-2-1, 2-2-2), with eight or nine abreast in economy (e.g., 3-2-3, 2-4-2, 3-3-3). Typical seat room ranges from 46 to 61 in (120 to 150 cm) pitch in first, 36 to 39 in (91 to 99 cm) in business, and 32 to 34 in (81 to 86 cm) in economy.



Mockup of early Dreamliner cabin concept

Cabin interior width is approximately 18 feet (547 cm) at armrest, 1 inch (2.5 cm) over what was originally planned, and 15 in (38 cm) greater than that of the Airbus A330 and A340, while 5 in (13 cm) less than the A350 and 16 in (41 cm) less than the 777. For economy class in 3-2-3 or 2-4-2 arrangements, seat-bottom widths will be 18.5 in (47 cm), comparable to that found on the Boeing 777, and recommended by detailed passenger ergonomics studies; for 3-3-3 and the 2-5-2 maximum passenger density layout, seat widths would be 17.18 in (43.55 cm), with most airlines expected to select the 3-3-3 maximum passenger density configuration. Boeing engineers designed the 787 interior to better accommodate persons with mobility, sensory, and cognitive disabilities.

For example, a 56-inch (142 cm) by 57-inch (145 cm) convertible lavatory includes a movable center wall that allows two separate lavatories to become one large, wheelchair-accessible facility.



Interior mockup photo showing windows and LED mood lighting options for the 787 Dreamliner.

The 787's cabin windows are larger in area than all other civil air transports in-service or in development, with dimensions of 10.7 by 18.4 in (27 by 47 cm), and a higher eye level so passengers can maintain a view of the horizon. Electrochromism-based "auto-dimming" (smart glass) instead of window shades reduces cabin glare while maintaining transparency. These are to be supplied by PPG Industries. Standard for the first time on a jetliner, cabin lighting uses light-emitting diode (LED) in three colors instead of fluorescent tubes, allowing the aircraft to be entirely 'bulbless' and have 128 color combinations.

The internal pressure will be increased to the equivalent of 6,000 feet (1,800 m) altitude instead of the 8,000 feet (2,400 m) on conventional aircraft. According to Boeing, in a joint study with Oklahoma State University, this will significantly improve passenger comfort. A higher cabin pressure is possible in part because of better properties of composite materials. Higher humidity in the passenger cabin is possible because of the use of composites, which do not corrode. Cabin air is provided by electrically driven compressors using no engine-bleed air. An advanced cabin air-conditioning system provides better air quality: Ozone is removed from outside air; HEPA filters remove bacteria, viruses, and fungi; and a gaseous filtration system removes odors, irritants, and gaseous contaminants.

Technical concerns

Composites



Disassembled composite fuselage section of the Boeing 787

The risks of using a composite fuselage have been questioned by a former Boeing engineer, noting that carbon fiber, unlike metal, does not visibly show cracks and fatigue; the rival A350 was later announced to be using composite panels on a frame, a more traditional approach, which its contractors regarded as less risky. Further concerns include that, during crash-landings, survivable in metal planes, a composite fuselage could shatter and burn with toxic fumes. The porous properties of composite materials, allowing them to absorb unwanted moisture, have been questioned. As the aircraft reaches altitude, the moisture expands, and may cause delamination of the composite materials, and structural weakness over time. Boeing has dismissed criticisms of its fuselage materials, insisting that composites have been used on wings and other passenger aircraft parts for many years, and they have not been an issue. They have also stated that special defect detection procedures will be put in place to detect any potential hidden damage. Another concern arises from the risk of lightning strikes, with composite having as much as 1,000 times less electrical conductivity than aluminum, increasing the risk of damage. Boeing has stated that the 787's lightning protection will meet FAA requirements, and FAA management was planning to adjust some requirements, which will help the 787 show compliance. In summer 2010, a 787 experienced an in-flight lightning strike without damage.

Weight issues

While Boeing had been working to trim excess weight since assembly of the first airframe began, common for new aircraft in development, the company has stated that the first six 787s will be overweight, with the first aircraft expected to be 5,000 lb (2,270 kg) heavier than specified. The seventh and subsequent aircraft will be the first optimized 787s and are expected to meet all goals, with Boeing working on weight reductions. Boeing has redesigned some parts and made more use of titanium. According to International Lease Finance Corporation's (ILFC) Steven Udvar-Hazy, the 787-9's operating empty weight is around 14,000 lb (6,350 kg) overweight, which also could be a problem for the proposed 787-10. In early 2009, a number of 787 customers started to publicly mention their dissatisfaction with the weight and range issues.



The first Boeing 787 at Paine Field

In May 2009, a press report indicated a 10–15% range reduction, about 6,900 nmi (12,800 km) instead of the originally promised 7,700 to 8,200 nmi (14,800–15,700 km), for early aircraft that were about 8% overweight. Substantial redesign work is expected to correct this, which will complicate increases in production rates; Boeing stated the early 787-8s will have a range of almost 8,000 nmi (14,800 km). There have also been reports that this led Delta to delay deliveries of 787s it inherited from Northwest in order to take later planes that may be closer to the original estimates. Other airlines are suspected to have been given discounts to take the earlier models. Shanghai Airlines stated in March 2009 it wished to either delay or cancel its first order. Boeing expects to have the weight issues addressed by the 21st production model.

Computer networks

In January 2008, previous FAA concerns came to light regarding protection of the 787's computer networks from possible intentional or unintentional passenger access. The computer network in the passenger compartment, designed to give passengers in-flight internet access, is connected to the airplane's control, navigation, and communication systems. Boeing called the report "misleading", saying that various hardware and software solutions are employed to protect the airplane systems, including air gaps for the physical separation of the networks, and firewalls for their software separation. Measures are provided so data cannot be transferred from the passenger internet system to the maintenance or navigation systems. As part of certification, Boeing plans to demonstrate to the FAA that these provisions are acceptable.

Variants



The Boeing 787-8, the first model of the aircraft under production

Boeing has offered three variants of the 787 from the program launch in 2004. The 787-8 is scheduled to enter service in 2011; the 787-9 is to enter service in 2013.

787-8

The 787-8 is the base model of the 787 family, with a length of 186 feet (57 m) and a wingspan of 197 feet (60 m) and a range of 7,650 to 8,200 nautical miles (14,200 to 15,200 km) depending on seating configuration. The 787-8 seats 210 passengers in a three-class configuration. The variant will be the first of the 787 line to enter service in 2011. Boeing is targeting the 787-8 to replace the 767-200ER and 767-300ER, as well as expand into new non-stop markets where larger planes would not be economically viable. The bulk of 787 orders are for the 787-8.

787-9

The 787-9 will be the first variant of the 787 with a "stretched" or lengthened fuselage, seating 250–290 in three classes with a range of 8,000 to 8,500 nautical miles (14,800 to 15,750 km). This variant differs from the 787-8 in several ways, including structural strengthening, a lengthened fuselage, a higher fuel capacity, a higher maximum take-off weight (MTOW), but with the same wingspan as the 787-8. The targeted date for entry into service (EIS), originally planned for 2010, was scheduled for early 2013 in December 2008. Boeing is targeting the 787-9 to compete with both passenger variants of the Airbus A330 and to replace their own 767-400ER. Like the 787-8, it will also open up new non-stop routes, flying more cargo and fewer passengers more efficiently than the 777-200ER or A340-300/500. The firm configuration was finalised on July 1, 2010.



Artist's impression of the stretched 787-9, designed with greater range and payload capability

When first launched, the 787-9 had the same fuel capacity as the other two variants. The design differences meant higher weight and resulted in a slightly shorter range than the 787-8. After further consultation with airlines, design changes were incorporated to add a forward tank to increase its fuel capacity. It will now have a longer range and a higher MTOW than the other two variants. The -9 will be able to fly non-stop from New York to Manila or from Moscow to São Paulo or Bogota to Sydney and will have the lowest seat-mile cost of the three 787 variants.

Air New Zealand is the launch customer for the 787-9 and the second customer ever for the 787 behind ANA. Qantas, Etihad Airways, and Singapore Airlines have placed the largest orders for the 787-9.

Other variants

787-3

This variant was designed to be a 290-seat (two-class) short-range version of the 787 targeted at high-density flights, with a range of 2,500 to 3,050 nautical miles (4,650 to 5,650 km) when fully loaded. It was designed to replace the Airbus A300/A310 and Boeing 757-300/767-200 on regional routes from airports with restricted gate spacing. It would have used the same fuselage as the 787-8, though with some areas of the fuselage strengthened for higher cycles. The wing would have been derived from the 787-8, with blended winglets replacing raked wingtips. The change would have decreased the wingspan by roughly 25 feet (7.6 m), allowing the 787-3 to fit into more domestic gates, in particular, in Japan. This model would have been limited in its range by a reduced maximum take-off weight (MTOW) of 364,000 lb (163,290 kg). (Actual range is based on remaining available weight for fuel after the aircraft empty weight and payload are subtracted from the MTOW.)



An artist's impression of the 787-3, which would have featured a shorter wing with winglets.

A full load of passengers and cargo would limit the amount of fuel it could take on board, as with the 747-400D. This is viable only on shorter, high-density routes, such as Tokyo to Shanghai, Osaka to Seoul, or London to Berlin. Many airports charge landing fees based on aircraft weight; thus, an airliner rated at a lower MTOW, though otherwise identical to its sibling, would pay lower fees.

Boeing has projected that the future of aviation between very large (but close) cities of five million or more may stabilize around the capacity level of the 787-3. Boeing also believed legacy carriers could have used this variant to compete with low-cost airlines by

running twice the capacity of a single-aisle craft for less than twice its operating cost (fuel, landing fees, maintenance, number of flight crew, airspace fees, parking fees, gate fees, etc.).

Forty-three 787-3s were ordered by the two Japanese airlines, but production problems on the base 787-8 model led Boeing to postpone the introduction of the 787-3 in April 2008, following the 787-9 but without a firm delivery date. By December 2009, all 787-3 orders had been converted to the 787-8. At the time, it was likely the 787-3 variant would be shelved entirely following the lack of interest by potential customers caused by its being designed specifically for the Japanese market. On December 13, 2010, Boeing did cancel the 787-3, since it was no longer financially viable after its orders were canceled.

787-10

Boeing has stated that it is likely to develop another version, the longer 787-10, with seating capacity between 290 and 310. This proposed model is intended to compete with the planned Airbus A350-900. The 787-10 would supersede the 777-200ER in Boeing's current catalog and could also compete against the Airbus A330-300 and A340-300. Boeing was having discussions with potential customers about the 787-10 in 2006 and 2007. This variant has not yet been officially launched by Boeing, but Mike Bair, at that time head of the 787 program, stated that "It's not a matter of if, but when we are going to do it ... The 787-10 will be a stretched version of the 787-9 and sacrifice some range to add extra seat and cargo capacity." The 787-10 has remained under consideration by Boeing.

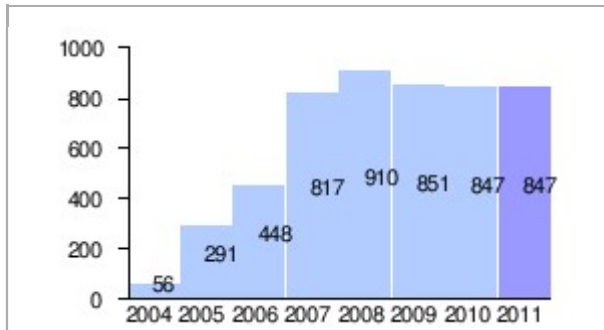
Further proposals

Although no date has been set, Boeing expects to build a freighter version, possibly in 10 to 15 years. Boeing is reported to be also considering a 787 variant as a candidate to replace the 747-based VC-25 as Air Force One.

Orders and deliveries

The Boeing 787 has not entered service. The first 787 is scheduled to enter passenger service in 2011 with All Nippon Airways. ILFC (International Lease Finance Corporation) is its largest customer ordering a total of 74 Boeing 787s, comprising 67 -8s and 7 -9s.

Net orders (cumulative by year)
--



Data through December 22, 2010.

Sources:

Boeing 787 total firm orders		
787-8	787-9	Total firm orders
621	226	847

- Data through December 19, 2010.

Orders and deliveries by year									
	2004	2005	2006	2007	2008	2009	2010	2011	Total
Net orders	56	235	157	369	93	-59	-4	0	847
Deliveries	-	-	-	-	-	-	-	-	-

- Data through December 22, 2010.

Specifications

Model	787-8	787-9
Cockpit crew		Two
Seating, typical	210-250 224 (3-class)	250-290 280 (3-class)
Length	186 ft (56.7 m)	206 ft (62.8 m)
Wingspan	197 ft 0 in (60.0 m)	197 ft 0 in (60.0 m)
Wing area	3,501 sq ft (325 m ²)	
Wing sweepback	32.2 degrees	
Height	55 ft 6 in (16.9 m)	
Fuselage dimensions	Width: 18 ft 11 in (5.77 m) / Height: 19 ft 7 in (5.97 m)	
Maximum cabin width	18 ft (5.49 m)	
Cargo capacity	4,822 cu ft (137 m ³)	6,086 cu ft (172 m ³)

	28× LD3 or 9x (88x125) pallets or 8x (96x125) pallets + 2x LD3	36× LD3 or 11x (88x125) pallets or 11x (96x125) pallets
Maximum takeoff weight	502,500 lb (228,000 kg)	545,000 lb (247,000 kg)
Maximum landing weight	380,000 lb (172,000 kg)	425,000 lb (193,000 kg)
Operating empty weight	242,000 lb (110,000 kg)	254,000 lb (115,000 kg)
Cruising speed	Mach 0.85 (567 mph, 490 knots, 913 km/h at 35,000 ft/10,700 m)	
Maximum speed	Mach 0.89 (593 mph, 515 knots, 954 km/h at 35,000 ft/10,700 m)	
Range, fully loaded	7,650–8,200 nmi (14,200–15,200 km; 8,800–9,440 mi)	8,000–8,500 nmi (14,800–15,700 km; 9,210–9,780 mi)
Maximum fuel capacity	33,528 US gal (126,920 L)	33,428 US gal (126,540 L)
Service ceiling	43,000 ft (13,100 m)	
Engines (×2)	General Electric GEnx <i>or</i> Rolls-Royce Trent 1000	
Thrust (×2)	64,000 lbf (280 kN)	71,000 lbf (320 kN)

Chapter- 8

Other American Inventions in 21st Century

Zostavax

Zostavax is a live vaccine developed by Merck & Co. which has been shown to reduce the incidence of herpes zoster (known as shingles) by 51.3% in a study of 38,000 adults aged 60 and older who received the vaccine. The vaccine also reduced by 66.5% the number of cases of postherpetic neuralgia and reduced the severity and duration of pain and discomfort associated with shingles, by 61.1%. Local reactions at the injections site were generally mild.

Zostovax was approved and licensed by the U.S. Food and Drug Administration (FDA) in May, 2006. The FDA recommended it only for adults 60 years of age or older who meet the following requirements:

- Has not had a life-threatening allergic reaction to gelatin, the antibiotic neomycin, or other component of the herpes zoster vaccine.
- Does not have a weakened immune system due to HIV/AIDS or another disease or medications (such as steroids, radiation and chemotherapy) that affect the immune system.
- Does not have a history of cancer affecting the bone marrow or lymphatic system, such as leukemia or lymphoma.
- Does not have active, untreated tuberculosis.

On October 25, 2006, the U.S. Centers for Disease Control and Prevention's (CDC) Advisory Committee on Immunization Practices (ACIP) voted to recommend that Zostavax be given to all adults age 60 and over, including those who have had a previous episode of shingles.

On 19 May 2006, the European Medicines Agency (EMA) issued a marketing authorisation for Zostavax for routine vaccination in individuals aged 50 and over.

Nanowire battery

A **nanowire battery** is a lithium-ion battery invented by a team led by Dr. Yi Cui at Stanford University in 2007. The team's invention consists of a stainless steel anode covered in silicon nanowires, to replace the traditional graphite anode. Silicon, which stores ten times more lithium than graphite, allows a far greater energy density on the anode, thus reducing the mass of the battery. The large surface area further allows for fast charging and discharging.

Design

Traditional silicon anodes were researched and dismissed due to the tendency of silicon to crack and become unusable because it swelled with lithium during operation. The nano-wires do not suffer from this flaw. According to Dr. Cui, the battery reached 10x density on the first charge and plateaued to 8x density on subsequent charges. In order to take advantage of this anode advancement, an equivalent cathode advancement is required to achieve the increased storage density.

Commercialization is expected to occur in 2012 with the batteries costing the same or less per watt hour than conventional lithium-ion batteries. The next milestone, life cycle testing, should be completed and the team expects to achieve at least one thousand charge cycles from nano-wire batteries.

In September 2010, Dr. Yi Cui's team demonstrated that 250 charge cycles are possible before the charge capacity drops below 80 percent of its initial storage capacity. The team expects to reach 3,000 charge cycles by 2012. Reaching this goal would make nano-wire batteries viable for use in electric vehicles. A prototype for use in cellular phones and other electronic devices is expected to be delivered by the first quarter of 2011.

Potential Problem

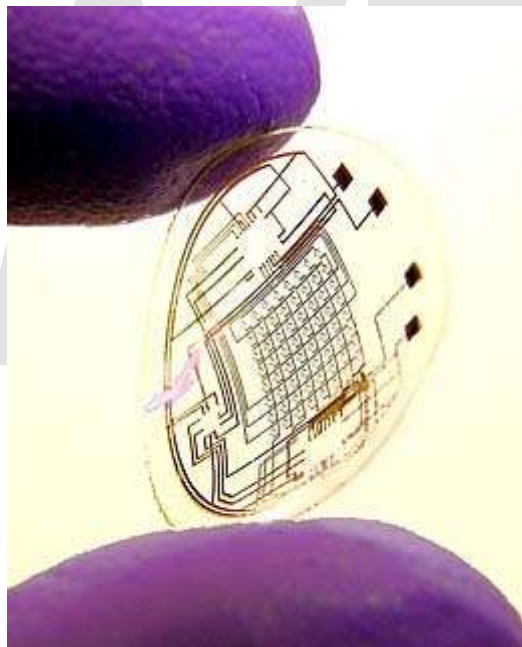
The very high surface area of the nanowires, which allows high charging rates, also has a downside: heterogeneous side reactions. These will occur as the nanowires on the negative electrode are brought below around +0.8 V, where the electrolyte becomes thermodynamically unstable and starts getting reduced. The result will be a film made from decomposition products that coats the surfaces of the nanowires. This coating, called a "solid electrolyte interphase (SEI)," is present in all Li-ion batteries that use conventional electrolytes and electrodes. Typically, the active particles on the negative electrode side (graphite) are around 10 microns in diameter. Even though such large sizes extract a penalty by lowering the surface area and power, that size is necessary in order to reduce the amount of SEI formed (which is proportional to the surface area). Even so, 5-10% of all of the Li in a Li-ion battery ends up incorporated into the SEI, leading to an irreversible capacity loss (ICL) of that amount. (The source of the Li in a cell is mainly the positive electrode, such as LiFePO₄.) Fortunately, the SEI formation reactions are self-limiting, and after the first cycle ICL can be very small.

On the other hand, a nanowire might have a couple of orders of magnitude more surface area per unit volume than a 10 micron particle, which would result in a couple of orders of magnitude more SEI formed--except that there is not enough Li in the positive electrode to make this much SEI. The result would be a drastic loss of capacity after the first cycle.

Nanowire cells can nevertheless be shown to cycle hundreds of times in half-cells. In a half cell, an electrode made from a piece of Li metal would be cycled against the nanowires, in which case there is an unlimited supply of Li. Therefore, capacity need never decline. Such half cells, however, would have no commercial value.

There are tricks that can be employed to reduce ICL--for example, by pre-forming the SEI before assembling the cell. However, this process is not done commercially because of the high cost of adding such a processing step.

Bionic contact lens



Picture of a bionic contact lens.

The **bionic contact lens** are being developed to provide a virtual display that could have a variety of uses from assisting the visually impaired to the video game industry. The device will have the form of a conventional contact lens with added bionics technology. The lens will eventually have functional electronic circuits and infrared lights to create a virtual display.

Babak Parviz, a University of Washington assistant professor of electrical engineering is quoted as saying "Looking through a completed lens, you would see what the display is generating superimposed on the world outside."

Manufacture

The lenses require organic materials that are biologically safe and also use inorganic material for the electronic circuits. The electronic circuits are built from a layer of metal a few nanometres thick. The light-emitting diodes are one third of a millimetre across. A grey powder is sprinkled onto the lens. Then a technique called microfabrication or 'self-assembly' is used to shape each tiny component. Capillary forces pull the pieces into their final position.

Development

Harvey Ho, a former graduate student of Mr. Parviz who is now working at Sandia National Laboratories in Livermore, California presented the results in January 2008 at the Institute of Electrical and Electronics Engineers' International Conference on Micro Electro Mechanical Systems (or microbotics) in Tucson, Arizona. The lens is expected to have more electronics and capabilities on the areas where the eye does not see. Wireless communication, radio frequency power transmission and solar cells are expected in future developments.

Prototype and testing

The prototype does not light up or display information; however, it is proof that it is possible to create a biologically safe electronic lens that does not obstruct a person's view.

Engineers have tested the finished lenses on rabbits for up to 20 minutes and the animals showed no problems.